UNIVERSITA' DEGLI STUDI DI NAPOLI FEDERICO II

DOTTORATO DI RICERCA IN INGEGNERIA
DEI MATERIALI E DELLE STRUTTURE

XXVII CICLO

DIPARTIMENTO DI INGEGNERIA CHIMICA, DEI
MATERIALI E DELLA PRODUZIONE INDUSTRIALE

MOLECULARLY IMPRINTED POLYMERS WITH ASSISTANT RECOGNITION BIOMOLECULE FOR PROTEIN DETECTION

TUTOR
Prof. Filippo Causa
Prof. Paolo Antonio Netti

CO-TUTOR
Dott. Edmondo Battista

DOTTORANDO
Nunzia Di Luise

Abstract

Molecularly imprinted polymers are ideal alternatives to natural recognition elements for a variety of reasons, including facile synthesis, greater chemical and long term stability, and reusability. One of the most challenging tasks in developing such polymers is provide them of a signal transduction capability, enabling to respond to a specific binding event. In this thesis, protein-imprinted polymers, capable of specific transduction of binding event into a fluorescence change were prepared using an assistant-peptide bearing an environment-sensitive fluorophore. The preparation has included the synthesis of the environment-sensitive peptide and subsequent incorporation into the polymer network through the imprinting process. Binding studies proved that MIP-SA-allyl-peptide has large absorption capacity and good affinity and selectivity toward BSA when compared with pure MIP. The greater binding properties of MIP-SA-allyl-peptide were found to derive from the assistant-peptide that suitably oriented into the cavity, acts as binding site in cooperation with the imprinted cavity. Furthermore, transduction signaling studies proved that MIP-SA-allyl-dansyl-peptide is able to detect and report the protein binding into a precise detection range. The proposed fluorescent-imprinted polymer provides a new and general strategy for protein-sensing platforms and opens up to the field of biosensors.

Acknowledgements

Table of Contents

List of Figures

List of Tables

Chapter 1. Introduction

1.1. Molecular recognition

1.1.1. Biomolecular recognition

Molecular recognition is a fundamental biological mechanism ubiquitous in nature. The ability to selectively recognize a target molecule in a vast pool of similar molecules is essential to biological and chemical processes. This elegant, and simple mechanism is found in nature in a number of processes, including antibody/antigen recognition in the immune system, enzyme/substrate binding, and nucleic acid interactions such as replication, transcription and translation [1]. Molecular recognition process is based on the formation of a complex between a receptor and a substrate, also called "lock-and-key" model that was firstly described by Fischer more than hundred years ago [2]. This model assesses that the formation of the complex is the result of intermolecular interactions between complementary functional groups on the lock (protein/enzyme) and the desired key (substrate). In other words, the two molecules must correspond both spatially and chemically [3]. Biorecognition relies on a complex orchestration of numerous interactions between individual atoms and cumulative interactions between secondary structures [4]. Such interaction is mostly based on non-covalent forces including ionic interactions, hydrogen bonding, van der Waals forces, π-π interactions and entropic considerations [5]. The sum of these

interactions, each of low energy on its own, leads to enormous specificity in binding [6]. For example, the active sites of enzymes are composed of several amino acid residues, which non-covalently bind ligand molecules in a very specific manner. However, the activity of the site is dependent on the stabilization of the three-dimensional structure by the interactions of hundreds of other residues within the structure of secondary and tertiary domains [4].

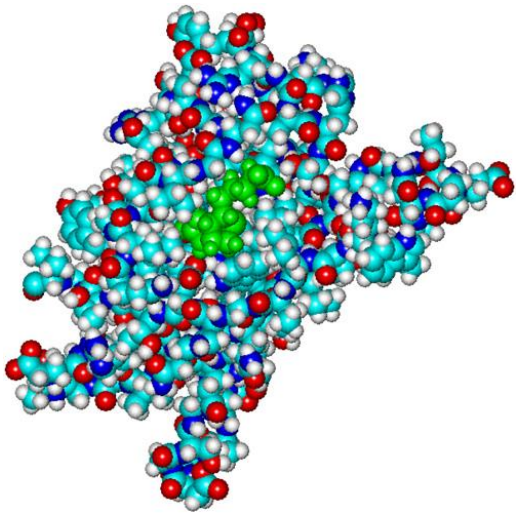

Figure 1. Complex between streptavidin and biotin, with biotin highlighted in green [6].

The complex between the vitamin biotin and the egg-white protein avidin (or the similar protein streptavidin from *Streptomyces avidinii*) illustrates the general principle of molecular recognition that has been routinely exploited by the nature. The dissociation constant for this complex is 10^{-15} M, one of the smallest ever measured for a non-covalent interaction between a protein and a small molecule [6, 7]. In table 1 typical biological dissociation

constants (K_D) of common classes of receptor-ligand interactions are reported.

	LIGAND	RECEPTOR	K_D (M)
CLASSES	Ligands	Macromolecules	$10^{-3} – 10^{-5}$
	Substrate	Enzyme	$10^{-3} – 10^{-6}$
	Carbohydrates	Protein	$10^{-3} – 10^{-6}$
	Steroid Hormones	Receptors at target tissue	$10^{-7} – 10^{-9}$
	antigen	IgG Antibodies	$10^{-8} – 10^{-10}$
SPECIFIC EXAMPLES	Glucose	Human Red Cell Gluocose Transporter, Glut1	$1.5 \cdot 10^{-2}$
	Fc Portion of Mammalian IgG	IgG antibodies	$5.2 \cdot 10^{-7}$
	Tri-peptide Inhibitor	Carboxypeptidase A	10^{-14}
	Pancreatic Trypsin Inhibitor	Trypsin	$6.4 \cdot 10^{-14}$
	Biotin	Streptavidin	10^{-15}

Table 1. Typical biomolecule receptor-ligand dissociation constants [4].

1.1.2. Biosensors

Molecular recognition is fundamental in biosensing. Mimicking the molecular recognition processes found in nature has always been paramount important for the scientific community because it opens up to several fields of applications ranging from biotechnologies to diagnostic tools and therapeutics. Recently, advances in the molecular level understanding of biological recognition processes together with the increasing of knowledge in integrated circuit technologies have led to a growing interest in the field of biosensors [8]. Since first seminal papers in the 1960s in which enzymes were used to detect biological compounds [9], several biosensors have

been studied and many techniques have progressively been associated to provide accurate detection of target analytes [10].

Higson and colleagues defined biosensor as “a chemical sensing devices in which a biologically derived recognition entity is couple to a transducer, to allow the quantitative development of some complex biochemical parameters” [11].

Turner described biosensor as a “compact analytical device or unit incorporating a biological or biologically derived sensitive recognition element integrated or associated with a physio-chemical transducer” [12].

In addition, according to a proposed IUPAC definition, “a biosensor should be clearly distinguished from a bio-analytical system, which requires additional processing steps, such as reagent addition. Furthermore, a biosensor should be distinguished from a bio-probe which is either disposable after one measurement, i.e. single use, or unable to continuously monitor the analyte concentration” [13].

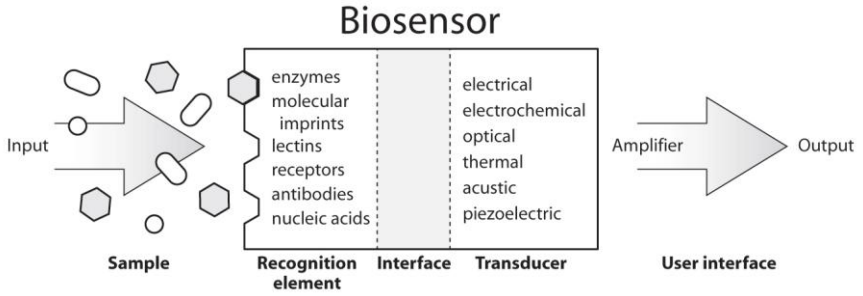

Figure 2. Schematic illustration of a biosensor.

Taking into account the different definitions, a biosensor is characterized by two main components: a recognition/sensing

element, which specifically interact with a target analyte, and a transducing element, which converts the interaction into a quantifiable effect (figure 2) [3].

The most approved recognition elements, based on antibodies, enzymes, receptors, nucleic acids and synthetic material will be extensively illustrated in the next paragraph.

Moreover, a variety of transducers have been studied, the most widespread include electrochemical, optical and piezoelectric [3].

Electrochemical biosensors measure the change that results from the interaction between the analyte and the sensing surface of the detecting electrode. The electrical changes can be based on: i) change in the measured voltage between the electrodes (potentiometric), ii) change in the measured current at a given applied voltage (amperometric), and iii) change in the ability of the sensing material to transport charge (conductometric). Due to their sensitivity, simplicity, low cost and fast response time, these sensors appear more suited for field monitoring applications such as clinical analysis, on-line control processes in industry or environment, and even *in vivo* studies [14, 8].

Optical biosensors transduce a biological event using an optical signal such as absorbance, fluorescence, chemiluminescence, surface plasmon resonance or changes in light reflectivity [15]. Although are advantageous for screening a large number of samples simultaneously, it is difficult to miniaturize them for insertion into the bloodstream as most optical methods still require sophisticated instruments [8].

Finally, **piezoelectric biosensors** are operated by applying an oscillating voltage at a resonance frequency of the piezoelectric crystal and measuring the change in this frequency when the analyte interacts with the crystal surface. Acoustic wave devices, including Surface Acoustic Wave (SAW) and Bulk Acoustic Wave (BAW) are the most common sensors, which bend when a voltage is applied to the crystal. Similarly to optical detection, piezoelectric detection requires large sophisticated instruments to monitor the signal [8].

Improvements in micro and nano-fabrication techniques, developments of new tools such as immunoreactions, conducting polymers, plasma polymerized films, bacterial magnetic particles as well as fundamental research for creating new devices (i.e. Surface Plasmon Resonance – SPR - microfluidic chip) will lead to an enhancement of biosensor properties in terms of miniaturization, specificity and sensitivity [10].

The rapid proliferation of biosensor technologies and the wide variety of devices have led to a lack of rigour in defining their performance criteria. Although each biosensor can only be evaluated for a particular application, it is useful to establish standard protocols for evaluating performance criteria in accordance with standard IUPAC protocols. These criteria include calibration characteristics (such as sensitivity, operational and linear concentration range, detection and quantitative determination limits), selectivity, steady-state and transient response times, sample throughput, reproducibility, stability and lifetime [16].

Biosensors technologies are applied in a wide range of fields for various purposes as environmental, food, clinical and national

security uses [3]. The largest biosensors sector is the medical/health area in which the glucose biosensors, including self-monitoring of blood glucose sensor and continuous glucose monitoring sensor are the most widely commercialized [10]. Furthermore, pharmaceutical industry requires biosensors to accelerate the processes of drug discovery and screening. Additionally, public safety has fostered developments in the environmental and food/agricultural industry promoting devices for the detection of pathogens and pollutants in foodstuffs [17].

1.1.3. Molecular recognition elements

Recognition elements, depending on the recognition properties of the biological component, can be classified in two broad families: catalytic and affinity-bases [18, 19]. The former family, also known as metabolism recognition elements, are kinetic devices where a biocatalyzed reaction is related to the concentration of the analyte. This family includes enzymes, microbes, organelles, plant or animal tissue or cells. In the latter, a binding event between a target molecule and a bioreceptor produces a physicochemical change that will be measured by the transducer. This family include antibodies, receptor proteins, nucleic acids, and molecularly imprinted polymers (MIPs) [10].

Initially, biosensor technology employed natural recognition elements as sensing materials; natural recognition elements were isolated from living system such as enzymes, microbes, antibodies, receptors, plant or animal tissues or cells [10]. An inherent advantage in the use of natural materials is the high affinity and specificity that is achieved as a result of a biologically optimized,

evolutionary process [19]. However, most of recognition elements now available are not naturally occurring but have been synthesised in the laboratory. Among the natural ones, bioengineered biomaterials are developed by engineering natural elements in order to improve such inherent advantages of natural materials [10]. Natural recognition elements, including enzymes, receptors, antibodies, aptamers, peptide nucleic acids (PNAs), will be briefly overviewed.

Receptors are attractive candidates as sensing materials and provide important opportunities for the development of biosensors for three principal reasons. First, because of their generic "receiving" and "sending" functions, receptors possess high affinity and specificity properties refined by the evolutionary process [20]. Second, receptors are natural targets for toxins, drugs and mediators of physiological processes, due to this they can be used for monitoring these compounds in clinical and environmental analyses and screening of drugs. Third, receptors are an important area of research as they can be useful for real-time elucidation of receptor-ligand interactions [19]. By conjunction of an environmentally sensitive probe in the proximity of the active site, environmental changes into fluorescence signals can be detected using a fluorescent system [21]. In the field of clinical and environmental sensors a number of attempts have been made to detect toxins. An example of this is a G-protein-coupled receptor, combined with an optical sensor based on fluorescent-labeled glycolipid receptor specific for cholera toxin [22]. Another one is ion channel protein, combined with a potentiometric sensor for detection of a wide

spectrum of toxins [19]. Although receptors possess interesting properties, a number of disadvantages limit their development as biosensors. Among them, low yield, high price, labour intensive isolation and lengthy purification protocols. Additionally, difficulty related to the transformation of the binding event into a processable signal, difficulty in the interpretation of the connection between signal formation and biochemical receptor function, are further drawbacks. Albeit progress in biotechnology techniques could reduce the price, nevertheless stability will remain an important factor that dramatically limits commercialization of receptors-based biosensors [19].

Enzymes are favoured components for the development of biosensors due to a variety of measurable reaction products arising from the catalytic process (protons, electrons, ions, light, and heat) [19, 20]. Additionally, unlikely receptors, enzymes offer an amplification effect due to the high level of catalytic turnover of these molecules and to the biochemical reaction products, allowing a direct monitoring of binding event [19] [23]. In most applications, the detection limit is satisfactory but the stability and thus the activity still remain challenging [24]. However, in order to improve biosensor performance such as lifetime and thermostability, several enzymes have been purified and engineered; water-soluble pyrroloquinoline quinone GDH was purified from *Klebsiella pneumonia* and engineered to improve thermostability by single amino acid replacement. [25]. Furthermore, the use of enzyme amplification to increase detection sensitivity is another important

issue; glucose oxidase can be combined with glucose dehydrogenase to significantly improve the response signal [26].

Antibodies are the most studied receptors responsible for specific recognition in nature [3]. Antibodies (also known as immunoglobulin) are large roughly Y-shaped glycoproteins produced by B cells and used by the immune system to identify foreign materials (antigens). Despite the complex milieu of biological fluids, antibodies bind to their target with exceptionally strong affinities with typical dissociation constants on the order of 10^{-8}-10^{-10} M [3]. Antibodies can be generated to a wide variety of target analytes, from whole bacterial cells to simple organic species [27]. In addition, novel technologies, including phage display antibodies libraries and recombinant antibodies permit the production even of analytes, which do not have a natural receptor [3]. Further, antibodies detection in complex matrices such as food, clinical, and environmental samples do not require time-consuming sample pre-treatments [20, 27]. Lastly, antibodies are relatively simple to immobilize and label using well-developed conjugation chemistry [27]. All these aspect, combined with their exceptionally strong affinity, selectivity and sensitivity makes the antibodies one of the most reliable recognition element in many biosensors [28]. Nowadays, antibodies are the mainstay of laboratory immunoassays and immunodetection techniques such as ELISA (enzyme-linked immunosorbent assay) and its variant ELISpot, western blotting, flow cytometry and immunofluorescent staining of cells and tissues [28]. These immunosensors have shown to be useful for detection of Hepatitis B and C, Simian immunodeficiency, Ebola, Rabies,

Epstein–Barr, and Measles viruses as well as biological agents such as botulinum neurotoxin A/B [29].

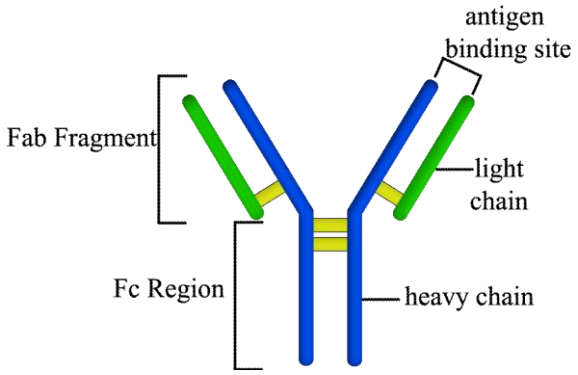

Figure 3. Y-structure of an antibody.

However, as most biological recognition elements, antibodies have inherent limitations mainly related to the stability, expensive and time-intensive synthesis, batch-to-batch variability, poor compatibility with transducers surfaces [3]. Nevertheless, stability, thanks to advances in recombinant DNA technologies, is being addressed by developing of new heat-stable, minimal sized single-domain antibody fragments derived from sharks and llamas, however these fragments typically show inferior solubility [27, 30]. The figure 3 illustrates Y-structure of an antibody

Aptamers are single-stranded nucleic acid ligands that are isolated from libraries of oligonucleotides by an *in vitro* selection process called SELEX (Systematic Evolution of Ligands by EXponential enrichment) [20, 31]. Unlike the preparation of antibodies, which relies on induction of an animal immune system, the SELEX process enables the fabrication of aptamers for non-immunogenic and toxic targets that it is otherwise impossible to obtain by the

immune system [32]. Thus, once selected, aptamers, can be synthesized with high reproducibility and purity from commercial sources [33]. Aptamers are thought to recognize their target primarily by shape (i.e. conformation) and not sequence [34]. In fact, since they are short and single-stranded oligonucleotides, these biomolecules possess the ability of folding into 3D structures conferring high affinity properties [20]. Predominantly unstructured in solution, the aptamers fold upon associating with the ligand into molecular architectures in which the ligand becomes an intrinsic part of the nucleic acid structure [32]. Since its discovery, a number of aptamers have been selected toward a broad range of targets, including metal ions, small organic molecules, peptides, proteins and whole cells. The primary limitation of the use of aptamers, specifically RNA aptamers, as recognition elements is their sensitivity to pyrimidine specific nucleases that are abundant in biological fluids. However, specific chemical modification of the ribose ring [35] of pyrimidine nucleotides results in significant stability and protection.

Peptide nucleic acids (PNAs) are synthetic DNA analogues or mimics with a polyamide backbone instead of a sugar phosphate bone. Of significant importance to biosensing, PNAs exhibit superior hybridization characteristics and improved chemical and enzymatic stability compared to nucleic acids [20].

Despite the success of systems based on natural recognition elements, they have inherent limitations that restrict their use. First, natural recognition elements have poor chemical, physical and long-term stability that allow their use just under aqueous conditions for

few days. Second, although labeling and immobilization techniques are well-established protocols, care must be taken to prevent blocking of the active site, resulting in loss of affinity. Third, the synthesis/preparation of natural recognition elements derives from complicated combinatorial processes that are time-consuming and skilled-labour, thus limiting large-scale production. In addition, batch-to-batch variability, cross reactivity between closely related target species and expensive analytical instruments are further issues [3, 27, 36]. However, because of their intrinsic high specificity and affinity, these natural recognition elements are the first popular choice in many biosensor applications. To date, antibodies are the most reliable recognition elements with the widest range of binding specificities [27].

1.1.4. Design of proteins and peptides

Attempts to develop bio-molecules with desired binding affinities for targets have lead to a growing interest in the design of proteins and peptides, including enzymes, receptors and antibodies. This approach provides new opportunities to develop novel biosensors with designed bio-macromolecules as recognition elements [37, 38]. Two primary approaches is being utilized, involving *de novo* design of binding pockets within well-folded protein structures and miniaturization of known protein binding motifs [38].

De novo design involves the construction of a protein intended to fold into a precisely defined 3-dimensional structure, with a sequence that is not directly related to that of any natural protein. This kind of approach represents the design in its purest and thus most challenging form [39]. In the second approach, the redesign of

naturally occurring protein is achieved by construction of "minimalist" sequences that are simpler than their natural counterparts but, nevertheless, retain sufficient complexity for folding and function [39, 40]. Both approaches are complementary and help define the minimum sequence requirements necessary for biomolecular recognition [38].

1.2. Peptides as recognition elements

1.2.1. Peptides as recognition elements

Miniaturized bio-macromolecules offer an alternative strategy to molecular recognition elements with selectivity and affinity properties comparable to their natural counterparts [38]. In this context, designed short peptides (up to 50 amino acids) are emerging as excellent opportunity for development of recognition elements for biosensor purpose. Short peptides represent a clear option for the design of synthetic receptors for a series of reasons: 1) the number of different peptides that can be obtained by the combination of the 21 natural amino acids is very much high; 2) the availability of both molecular biology and chemical techniques for the fast screening of peptide libraries is less time-consuming; 3) the automated synthesis and purification technologies, compared with the technologies for the preparation of monoclonal antibodies, are much easier; 4) the ease of modifications in a site-specific manner allows for fluorophore coupling and immobilization on solid support; 6) the relatively easy modeling permits more accurate computation studies.

A growing number of biomimetic, peptide-based sensing systems have been reported in the recent literature, and a wide range of target analytes includes whole cells, proteins, small organic molecule and ions [41].

1.2.2. Selection and synthesis strategies for peptide-based sensors

In the recent years, peptide-based sensors have been developed according to different strategies.

Synthetic design peptides have been designed on the basis of known interactions between single or few amino acids and targets, with attention being paid to the presence of peptide motifs known to allow intermolecular self-organization of the peptides over the sensor surface. Sensitive sensors have been obtained in this way for ions, small molecules and proteins (figure 4).

Short peptides from random phage display have been selected in a random way from large, unfocussed, and often preexisting and commercially available libraries with no design element. Such peptides often perform better that antibodies, but they are difficult to select when the target is a small molecule because of the need to immobilize it with considerable modifications of its structure.

Peptide receptors for ligand sensing are artificial, miniaturized receptors obtained from reduction of the known sequence of a natural receptor down to a synthesizable and yet stable one.

Finally, **peptide ligands for receptor sensing** are short peptides that have been used as active elements for the detection of their own natural receptors: pathogenic bacteria have been detected with antimicrobial and cell-penetrating peptides. However, key

challenges such as detection of bacteria in real samples, improved sensitivity and selectivity have to be faced [41].

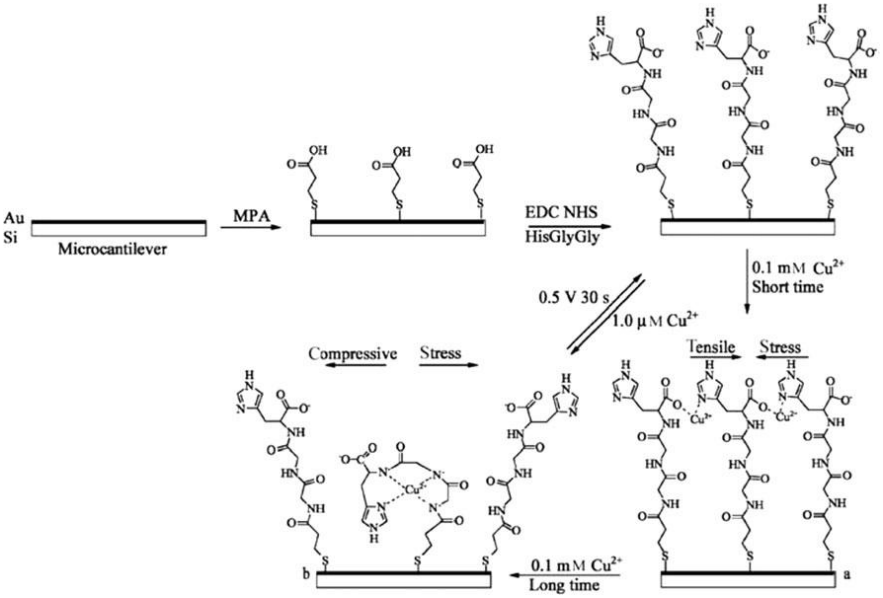

Figure 4. Selective binding of copper to a microcantilever coated with a tripeptide [41].

1.2.3. Peptide-based fluorescent biosensors

The development of peptide-based sensors over the last two decades has been spectacular. Fluorescent techniques, due to their high sensitivity, selectivity, fast response time, flexibility and experimental simplicity have dominated the field. FRET (Fluorescence Resonance Energy Transfer) effects or environment-sensitive fluorophore provide reliable design strategies that can be safely implemented to study virtually any biological interaction with minimal efforts [21].

Environment-sensitive fluorophores (figure 5) are molecules that display emission properties that are responsive to the

physiochemical changes in their immediate surroundings [21]. Physiochemical changes include pH, viscosity, biological analytes and solvent polarity. By conjugating these probes to a molecule (i.e. protein), it is possible to obtain valuable information regarding the state of a protein with high spatial and temporal resolution [42].

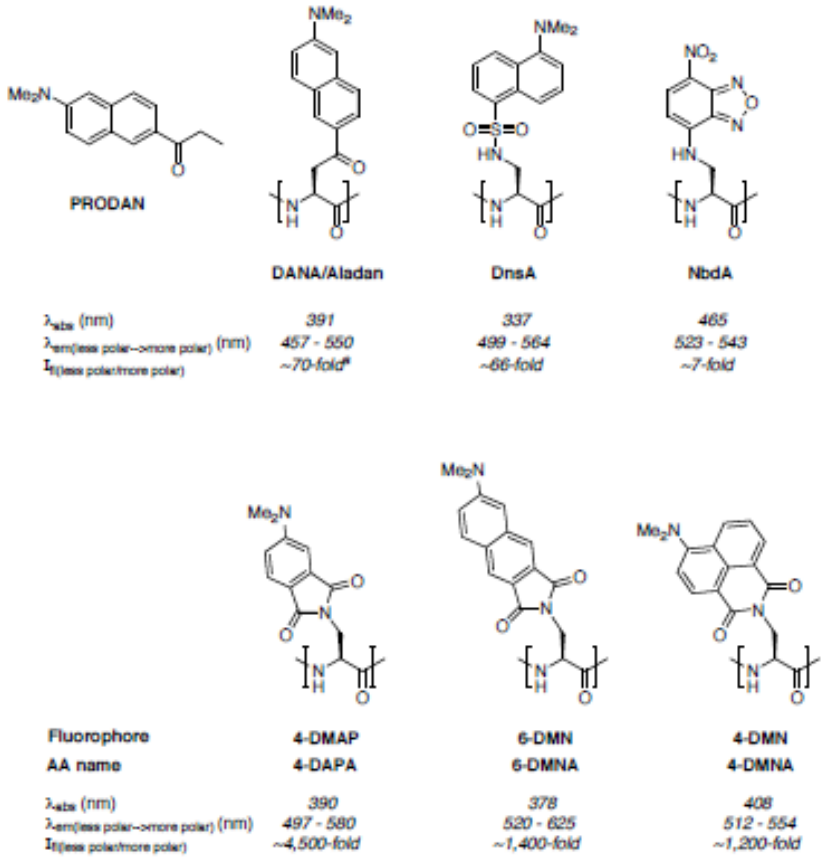

Figure 5. Comparison of some environment-sensitive fluorophores and their solvachomatic properties [43]. Abbreviations: 4-DMNA: 4-(N,Ndimethylamino) naphthalimide alanine, 6-DMNA: 6-(N,N-dimethylamino)-2,3-naphtalimide alanine, DANA/Aladan: 6-(2-dimethylamino)-naphthoyl alanine, 4-DAPA: 4-(N,N-dimethylamino)-phalimido alanine, 4-DMAP: 4-(N,N-dimethylamino) phthalimide, DnsA: Dansyl alanine, TAMRA: 5-(and-6)carboxytetramethyl rhodamine, 6-DMN: 6-dimethylamino-1,8-naphthalimide, 4-DMN: 4-dimethylamino-1,8-naphthalimide, NbdA: 7-nitrobenzo-2-oxa-1,3-diazole.

Key physical parameters include extinction coefficients, excitation and emission wavelengths, quantum yields, size hydrophobicity, and stability. Indeed for specific applications, it is often challenging to identify a species that possess all of the desired attributes [42].

Two main strategies for covalent incorporation of a fluorophore in the peptide can be distinguished. The first one involves post-synthetic coupling at the N-terminal or at the side chains of cysteines or lysines. The second one uses unnatural fluorescent amino acids for peptide synthesis [44]. However the insertion of the fluorophore is restricted topologically to sites in the protein that preserve function and activity while permitting the dye to make necessary contacts that result in measurable fluorescence changes. This consideration necessitates the use of methods that offer precise control over dye placement within peptide, with minimal perturbation [42].

The figure 6 illustrates the general principle of a fluorescent peptide biosensor, while table 2 summarizes environmentally sensitive peptide biosensors.

Fluorescent sensor peptides have proven useful in a number of applications, ranging from analyte detection to elucidation of molecular details of protein-peptide and protein-protein interactions. It is expected that their general applicability with respect to analyte quantification will be expanded by combining combinatorial methods for peptide design with further improvements of fluorophores and fluorescent amino acids in terms of sensitivity to environmental changes [44].

Figure 6. General principle of a peptide-based fluorescent biosensor that use environment-sensitive fluorophore as signaling mechanism of interaction with the target protein [21]

ANALYTE	RECEPTORS	FLUOROPHORE
DNaK chaperone	Targeting sequence of precursor of aminotransferase	Acrylodan
Cholecystokinin (CCK) receptor	Peptides agonist of the CCK receptor	Alexa 488
α-amilase	Library of designed loop peptides	fluorescein
Calmodulin	Library of designed α-helical peptides	TAMRA
Double-stranded DNA	Polypeptide derived from the Hin recombinase of *Salmonella typhimurium*	Oxazole yellow
Opioid-receptor	Opioid antagonist	DANA (Aladan)
Class II MHC proteins	HLA-DR-binding peptides	4-DAPA and 6-DMNA

Table 2. Selected environmentally sensitive peptide biosensors [44].

1.3. Molecularly imprinted polymers

1.3.1. Molecularly imprinted polymers

The typical weaknesses of natural recognition elements, the advances in protein chemistry as well as the increased understanding of protein recognition, have led researchers to investigate alternative synthetic receptors that can specifically bind target molecules with affinity and selectivity similar to those of the

fragile biological elements. A promising approach that recently has gained significant interest is molecular imprinted polymers (MIPs) [1]. The “molecular imprinting” concept was firstly proposed by Polyakov in 1931 as “unusual adsorption properties of silica particles prepared using a novel synthesis procedure”. It was the first report in which selectivity was due to a template effect, although the additives, acting as template, were included after polymerization [45]. However, the idea of molecular imprinting was inspired by the theories of Pauling on the formation of antibodies in the immune system [46, 47]. Pauling theorized that antibodies behaved like denatured proteins and thus their chains were free to move. When in contact with an antigen, chemical functionalities on the antigen would attract amino acids on the antibody, a mechanism he termed ‘‘molecular complementariness’’. Thus the antibody would then memorize the shape of the antigen [47]. This hypothesis was later disproved, but his idea of a freely moving polymer chains that could form a complementary mold around a structure inspired the field of MIPs [1].

Molecular imprinting is a technique in which a polymer network is formed with specific recognition for a desired molecule [3]. The process of molecular imprinting involves the formation of recognition cavities through connecting of different building blocks under the guidance of a analyte molecule that acts as a molecular template [36]. In other words, molecular imprinting can be defined as a process of template-induced formation of specific molecular recognition sites in a material where the template directs the positioning and orientation of the material’s structural components

by a self-assembly mechanism [48]. The figure 7 illustrates the principle of the molecular imprinting technique.

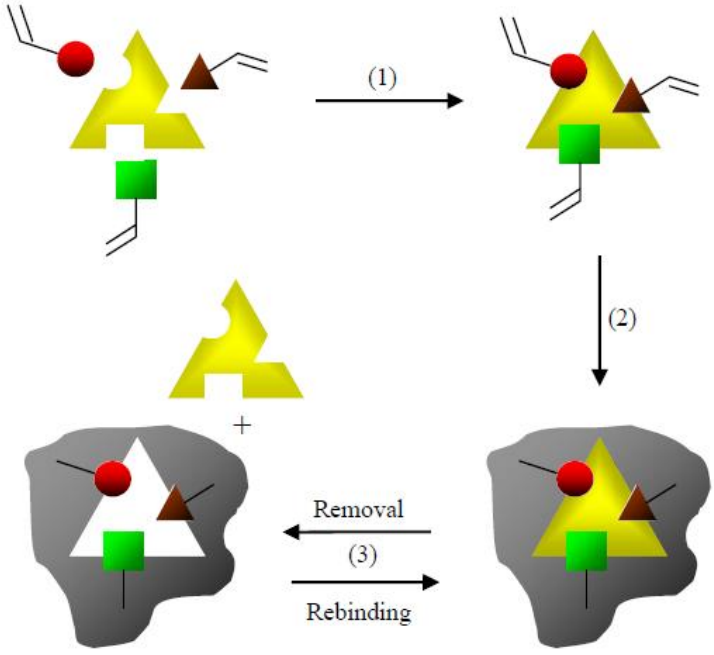

Figure 7. Molecular imprinting: (a) Formation of a pre-polymerization complex with template (yellow) and functional monomers (red, green and brown) by interactions that occur between complementary functionalities in the template molecule and functional monomer units. (b) Polymerization with cross-linking agent to produce the MIP (grey); (c) Template removal which leaves specific recognition sites that are complementary to the templates in terms of size, shape and chemical functionality orientations, thus enabling subsequent recognition of the template during the rebinding process [52].

In a general MIP polymerization procedure a solution of appropriate functional and cross-linking monomers in identified, a desired template molecule is added, and the solution is mixed. This mixing allows for a pre-polymerization complex of the template molecule with the complementary monomers [36]. To date, functional monomers are chosen to exhibit specific chemical structures designed to interact with the template via covalent, non-covalent

chemistry or both [49]. Once the pre-polymerization complex is formed, the monomers are polymerized; subsequent removal of the template from the as-formed polymer reveals a porous matrix with specific cavities for the template molecule [1]. These cavities are three-dimensional binding sites with stereochemical complementarity to the template molecule of interest. The position and arrangements of functional groups within these binding sites constitute an induced molecular memory. As such, during the subsequently rebinding process, the host-guest interactions within the molecular imprinting system are comparable to some typical biosystem, such as receptor-ligand, antibody-antigen and enzyme-substrate [50, 51].

1.3.2. Imprinting approaches

In the molecular imprinting, as explained above, the pre-polymerization complex between the functional monomers and the template determinates, following the polymerization, the formation of an imprint of the template [50]. Various driving forces are implicated in the pre-polymerization complex, including covalent bonding, hydrogen bonding, van der Waals forces, ionic interactions, metal coordination interaction and hydrophobic effect. According to the involved interactions, two different approaches have been followed for obtaining molecularly imprinted polymers [36].

In the covalent approach, first developed by Wulff, the template is bound covalently to functional monomers and the same interactions are used by the MIPs to bind the template. In principle, this

approach can lead to homogeneous binding site, since the template-functional monomer complex can be kept intact during the polymerization. However, removal of the chemically bounded template from the polymer matrix as well as rebinding is difficult to achieve [36].

The non-covalent approach, first reported by Mosbach, [53] mimics the interactions prevailing in biomolecular recognition process. In this approach, functional monomers and template are mixed in a proper solution and upon mix, they "self-assemble" to form the complex. Once polymerized, the template can be removed via simple diffusion in a proper solvent that overcome the non-covalent interactions [1]. Because of the relatively weak interactions involved, an excess of functional monomers is often added in order to stabilize the complex which can result, however in heterogeneous binding sites [36]. Due to its simplicity, most of the imprinting procedures, especially in imprinting biomolecules, deal commonly with this approach [49]. Consequently, the design imprinting optimization studies discussed later will covers mainly non-covalent approach. A comparison between covalent and non-covalent imprinting approach is resumed in table 3.

	IMPRINTING APPROACH	
	COVALENT	**NON-COVALENT**
Synthesis of monomer-template conjugate	necessary	unnecessary
Polymerization conditions	rather free	restricted
Removal template after polymerization	difficult	easy
Template binding and release	slow	fast
Structure of template binding site	clearer	less clear

Table 3. Comparison of covalent and non-covalent imprinting approach.

1.3.3. Imprinted molecules

Molecular imprinting technique has a considerable potential in broad areas of applications ranging from clinical analysis, medical diagnostics and drug delivery to environmental monitoring [54]. Various template have been successfully exploited and used (sugars, steroids, pesticides, drugs, amino acids derivatives), leading to significant achievements in the areas of analytical separation, solid phase-extraction, electrophoresis, artificial enzymes, chemical sensors, drug delivery and library screening tools [52]. Among all the templates, small molecule (molecular weight < 1500 Dalton), have dominated in the synthesis of MIPs and a number of companies now sell tailor-made imprinted products (MIP Technologies AB, POLYIntell, and Semorex) [6].

In contrast, progress in imprinting larger and more complex templates, such as macromolecules (molecular weight > 1500 Dalton), is slow and it still represents a challenging task [50, 54]. Imprinting macromolecules has a great potential mainly in biomedical and diagnostic area. In the laboratory settings, the use of a cheap and reusable tool would be useful in the isolation, extraction and purification of proteins in assays, replacing the current immunoassays techniques that utilize antibodies [3]. Further, removal/neutralization of toxic bio-macromolecules in the body as well as targeted therapeutic delivery devices are others potential applications [3]. Proteins, DNA, whole cells and carbohydrates are the typical bio-macromolecular targets for imprinting, however due to their relevant importance in the biological systems, proteins are the most extensively studied

templates [50]. A comparison of the MIPs to natural recognition elements is shown in table 4.

	NATURAL RECOGNITION ELEMENTS	**MIPs**
Binding affinity	High affinity/specificity	Varies (especially for macromolecular templates)
Generality	One receptor for analyte	MIPs can be developed for any template
Robustness	Limited stability	Stable in variety of conditions (pH, T, ionic strength, solvents)
Cost	Expensive synthesis but cost-effective	Inexpensive
Storage	Days at room temperatures	Long term storage without loss in performance (several months to years)
Synthesis/preparation	Time-intensive	Facile
Sensor integration	Poor compatibility with transducer surfaces	Fully compatible
Infrastructure required	Expensive analytical instruments/skilled labor	Label-free detection

Table 4. Comparison of natural recognition elements with MIPs [3].

Of note is the fact that MIPs have many advantages over antibodies in terms of their overall stability, ease of synthesis and use, as well as facile integration with transducers. However, at this point MIPs are not able to directly compete with the binding affinity and selectivity demonstrated by natural recognition elements, especially for current applications where antibodies are used in their soluble form [3].

1.3.4. Obstacles to imprinting proteins

The bottleneck in imprinting proteins relies in the natural properties of proteins: size, complexity conformational instability and solubility [52]. Firstly, proteins are water-soluble compounds that are not always compatible with the conventional imprinting procedures which rely on using aprotic organic solvents for the polymerization [54]. Second, as proteins are macromolecules, they can remain entrapped in the network after polymerization and cannot easily diffuse back in the subsequent rebinding. Network diffusion limitations, in both directions, lead to inadequate recognition properties [3]. Thirdly, proteins are complex bio-polymers composed of a linear sequence of amino acids (primary structure) that present a large number of chemical groups potentially available for the interaction with functional monomers; different portions of the protein exhibit distinct chemical groups. This complexity leads proteins to having multiple weak interactions that increase the probability of non-specific binding [52]. Fourth, in addition to the primary structure, proteins have a secondary (folding, α-helix, β-sheets, loops), tertiary (disulphide bonds) and quaternary (multimers of individual molecules) structures that make them very flexible. As polymerization conditions employed during the imprinting procedures are usually non-physiological, changes in protein structure lead to different conformations than those found in natural environment, causing the resultants binding sites to be specific to this altered non-natural state [3, 50].

1.3.5. General strategies to macromolecular imprinting

Despite several obstacles, many researchers have attempted to imprint macromolecules through a variety of different imprinting protocols. These imprinting protocols differ mainly in type and amount of functional monomers, model template, crosslinking monomer as well as solvent and polymerization reaction [55]. The optimization of the mixture composition will allow for an appropriate polymer matrix, with high affinity binding sites, and virtually without aspecific interactions [56]. In addition, four main imprinting approaches, mostly categorized as bulk, particles, surface and epitope, have been reported [3].

The following two paragraphs overview the most commons strategies to optimize the mixture composition as well as the general imprinting approaches to macromolecular imprinting.

1.3.5.1. Composition mixture optimization

In the imprinting process the **template** is of central importance as it directs the organization of the functional groups pendant to the functional monomers [57]. In a non-covalent imprinting approach, templates with more and diverse chemical functionalities are, in theory, easier to imprint [55]. Hydrogen bond donating moieties and electrostatic functionalities (carboxyl, amino, hydroxyl, and amide) are some of the most commonly chosen sites on a template molecule [1]. These chemical functionalities can form multiple non-covalent bonds producing a very stable binding complex with the functional monomers. However, protein templates that possess a very complex structure can bear polymerizable chemical groups that

can participate in the polymerization, resulting in crosslinking of the protein in the polymer [55]. An exhaustive analysis of the literature reveals that almost all reports employ a number of well defined, relatively stable and inexpensive model proteins as template (albumin, hemoglobin, lysozyme), illustrating that imprinting of macromolecules is still in its initial phase of development, mostly focused on demonstrating the proof of concept [56].

Once selected the template, the choice of the functional monomers that selectively assembly with the template creating high affinity binding sites is paramount to a successful imprinting [56]. The number, diversity and amount of functional monomers that interact with the template, the strength of the monomer-template interactions, as well as the monomer reactivity ratios determine the performance of the imprinted polymer. The strength of the monomer-template complex is crucial, as the polymer is forming, any cross interactions between the solvent and the monomer-template complex can affect the imprinting efficacy [55]. Thus, there is always a trade-off in using weak/neutral or strong/charged binding monomers [54]. However, it has been proposed that multiple weak interactions between monomers and template are necessary for the generation of a strong-protein binding polymer network in aqueous environment [56]. Hjertèn and co-workers firstly introduced acrylamide (Aam) and N,N'-methylene-bisacrylamide (MBA) to create MIPs for recognition of several proteins: cytochrome C (Cyt C), hemoglobin (Hb) [58], ribonuclease (RNase), human growth hormone [59] and human serum albumin (HSA) [60]. Mix of the monomers at different ratios

were used to pack chromatographic columns and tested for their binding affinity. The results showed that polymers had high recognition properties, even capable to discriminate between two homologous proteins [59]. By incorporating chargeable functional monomers in the polymeric backbone led Hjerten and co-workers to a decreased selectivity toward hemoglobin concluding that the use of charged monomers should be avoid. However, in some cases, the use of a chargeable monomer, such as acrylic acid (AAc) for the imprinting of lysozyme, has demonstrated to be useful [61] and in some cases even essential [62]. Lysozyme was also successfully imprinted by Zang by using only neutral monomers, showing that surface charge on the polymer is not necessarily needed [63].

The amount of functional monomer as well as the amount of crosslinker are others important issues to be considered. **Total monomer concentration** (T%) and **crosslinking density** (C%) are two parameters useful to optimize the polymer composition. T% is defined as the total monomer plus crosslinker expressed as a % w/v. T% dictates the average length and thus molecular weight of the linear polymer chains. C% is defined as the weight percentage of total monomer and dictates the extent of crosslinking. Variation of C% and T% enables the creation of polymer matrix with different recognition properties and physical characteristics (pore size, elasticity, density, and mechanical strength) [64].

Moreover, the **functional monomer to template ratio** (M/T) is another key parameter in a successful imprinted polymer. In the non-covalent approaches, usually, in order to push the reversible functional monomer-template interactions to the complexed state,

an excess of functional monomer is needed. The optimum M/T ratio can be distinctively seen by looking at two extreme cases: at very large M/T ratio, the monomers incorporation within the polymer chains are highly randomly and there is no difference between the imprinted and non-imprinted polymer whereas at a very small M/T ratio there are not effective multiple monomer interactions with the template, resulting in no recognition. [55]. The work of Alvarez-Lorenzo and of Hjratani has deeply analyzed this aspect of the imprinting [65].

The diversity of functional monomers is also a variable; a work of Venkatesh proves that the loading of the drug into networks containing four different functional monomers is 6 and 3 times greater than control network and networks containing 2 or 3 functional monomers, respectively [66]. This achievement suggests that multiple non-covalent bonds produce a very stable binding complex such as those found in natural recognition systems [67]. Additionally, when two or more functional monomers are used simultaneously, in order to ensure that co-polymerization is feasible, it is important to take in account the reactivity ratios of the monomers as well as cross interactions. [57].

Scores of functional monomers with chemically diverse structures and polarities are commercially available and many more can be prepared by rational design [57]. However, an exhaustive analysis of the literature reveals that the majority of the studies employ polyacrylamide gel and derivates using Aam and MBA as functional and crosslinking monomer, respectively. The advantages in using this polymer gel are: inertly with non-specific serum

protein adhesion, well-known polymerization mechanism, excellent biocompatibility *in vivo*, formation of the gel under a wide range of temperature and pH, and a multitude of procedures already present in literature [64].

TEMPLATE	COMPONENTS	XL mol%, M/Tmolar ratio
LYS	MAH, HEMA, EGDMA	650MAH:1LYS
HSA	Aam, MBA	2.4mol%MBA, 371000:1
LYS, Cyt C	NiPAam, MAA, Aam, MBA	1.3% MBA, 250:1
BSA	DMAPMA/Aam/NiPAam, MBA	3mol%MBA 2450:1
BSA	DMAPMA, TEGMDA/PETTA	9mol% 7970:1
BSA	Sodium alginate, $CaCl_2$	n/a
RNase A, BSA, LYS	MMA, EGDMA, surfactant (SDS, PVA)	75mol% 4000:1
Trypsin	Methacrylamide, EBA, methacryloylaminobenzamine	60%
Albumin	DMAPMA, TEGMDA/TMPTMA/PETTA, Au electrode	90% 250:1
RNaseA, LYS, Myoglobin, OVA, CRP	Styrene, MMA, MAA, DMAEMA, 4VP, HEMA, various PEG(n)DMA	30-75%
Cyt C	Aam, mica, MBA/EBA/PDA/or PEGDMA	3,3%
Angiotensin II, SA(octapeptide)	Na acrylate, PEGDA, MAA, EGDMA	86-96% PEGDA 8:1-32:1
Epitopes for Cyt C, ADH, BSA	Aam, MBA, PEG(200)DA	33%

Table 5. Selected MIPs for a large variety of proteins with the associated composition edited from [3]. Abbreviations: HEMA: 2-hydroxyethyl methacrylate, EGDMA: ethyleneglycol dimethacrylate, NiPAam: N-isopropyl acrylamide, MAA: methacrylic acid, DMAPMA: 3-dimethylaminopropyl methacrylamide, TEGMDA: tetra(ethyleneglycol) dimethacrylate, PETTA: pentaerythritol tetraacrylate, MMA: methyl methacrylate, SDS: sodium dodecyl sulphate, PVA: poly(vinyl alcohol, EBA: N,N-ethylenebis(acrylamide), 4-VP: 4-vinyl pyridine, PEG(n)DMA: poly(ethylene glycol) (n) dimethacrylate, PDA: 1,4-bis(acryloyl) piperazine, PEG(200)DA: polyethylene glycol (200) diacrylate, CRP: C-reactiv protein.

The table 5 summarized a selective MIPs for a large variety of protein templates with the associated composition and selectivity. Of note is the fact that each MIPs have a unique polymerization mixture demonstrating that macromolecularly imprinting is still a highly empirical technique [6].

1.3.5.2. Imprinting approaches

Apart the polymer composition, four main approaches have been proposed for macromolecularly imprinting - bulk, particle, surface, and epitope.

Bulk imprinting (figure 8): the standard technique for the small-molecular weight templates is the most straightforward approach to macromolecularly imprinting. The advantages to this approach are that three-dimensional binding sites are formed for the entire protein and that there are a multitude of facile procedures already present in literature. However, a few inherent obstacles can difficult this strategy, including diffusional limitations, solubility concerns of the template in organic solvents often used in small molecules imprinting, and conformational changes in the protein template caused by the non-physiological conditions employed. The majority of bulk imprinting involves wet sieving or crushing the polymer after polymerization and before template removal. However, this approach produces irregularly shaped and polydisperse particles and may destroy potential binding sites [3].

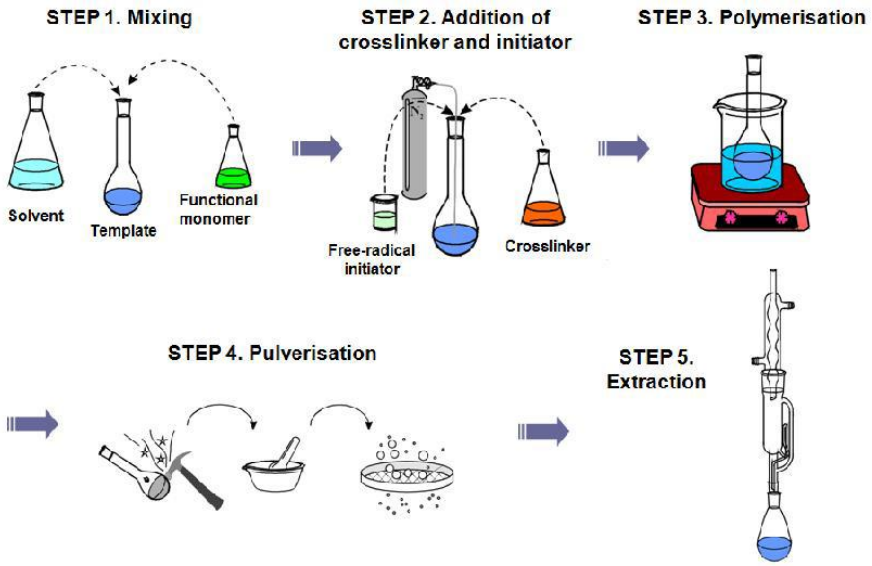

Figure 8. Schematic representation of bulk imprinting approach.

As a result, various groups have explored the possibility to directly synthesize micro/nano-particles as platform for imprinting.

The main differences between bulk and **particle imprinting** are the addition of stabilizers/surfactants and the much lower monomer/template concentrations in the pre-polymerization solution. Drawbacks to this method are that residual amounts of stabilizers may remain in the polymer particles even after extensive washing as well as the potential disruption of the monomer-template complex due to the presence of surfactants [3].

In the **surface imprinting**, the binding sites are located at or very near the surface of the polymer. This is achieved either synthesizing a thin polymer film or by attaching the protein template on the surface of the substrate (flat or spherical) with subsequent polymerization. As the binding sites are near the surface, this method facilitates diffusion of the macromolecules into and out of

the network. Additionally, surface imprinted MIPs tend to be more physically robust due to the presence of the support and allow for easier sensor integrations. However, as only a portion of the protein is imprinted, a decreasing in specificity is often observed [3].

Combining the concepts of surface and bulk imprinting, the **epitope imprinting** (figure 9) employs a short polypeptide as the template during polymerization to represent a moiety of a larger molecule template ultimately desired to be recognized. The resulting polymer is able to recognize not only the short peptide template but also the entire protein [52, 68].

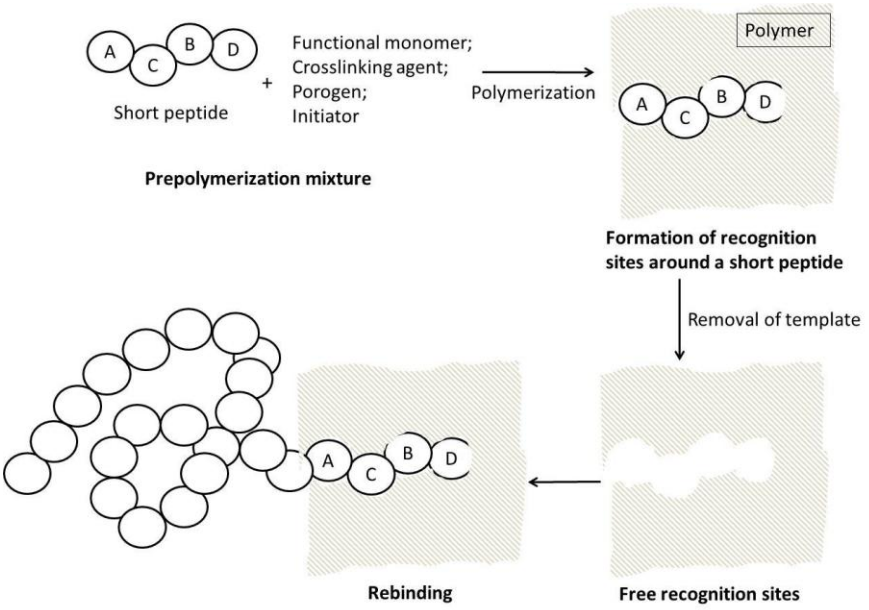

Figure 9. Schematic representation of epitope imprinting approach.

This technique attempts to more closely mimic the specific interaction between an antibody and antigen described earlier. Epitope imprinting has several advantages. First, more specific and stronger interactions with a small part or fragment of the protein can

minimize non-specific binding and improve affinity. Second, organic solvents can be employed for the polymerization process, because small peptide templates are more stable in these solvents [3]. Table 6 summarizes the four main imprinting approaches for macromolecularly imprinting.

IMPRINTING APPROACH	TEMPLATE	MONOMER COMPOSITION
Bulk	Hb	Polyacrylamide-chitosan beads complex
	LYS	Hydrogel
	BSA, urease, Hb	Polysiloxane
Particles	BSA	Sodium Alginate
	RnaseA, BSA, LYS	Polymethylmethacrylate
	Amylase	Poly(ethylene-co-vinyl alcohol)
Surface	LYS, RibonucleaseA, myoglobin	Polymethacrylate
	Hb	Polysiloxane-silica complex
	Horse spleen ferritin, BSA	Ternary lipid monolayer
Epitope	Short peptides	Polyacrylamide
	C-terminal protected phosphorylated short peptide (FmocTyr(PO3H2)-Pro-OH)	Polymethacrylamide
	N-and C-terminal protected phosphorilated tyr	Polymethacrylate

Table 6. Summary of selected examples of MIPs using bulk, particle, surface and epitope imprinting approach edited from [3, 52].

The works discussed above clearly demonstrate that MIPs can bind proteins specifically and with high affinity. In particular, four imprinting approaches emerge as general strategies. However, the multitude of different protocols and approaches to the macromolecularly imprinting, highlight the need for a systematic

and through optimization of the type and relative amounts of functional and crosslinking monomers as well as of all components of the imprinting mixture.

1.3.6. Alternative macromolecularly imprinting strategies

The success of an imprinted polymer lies with the monomer-template complex [1]. This complex must be thermodynamically favorable and stable under reaction conditions, but at the same time the bonds must be easily broken for subsequent template removal such that the binding sites are not disturbed. The dominant recognitive forces in macromolecularly imprinted polymers are typically non-covalent interactions. As result, researchers have focused their efforts toward the optimization of the pre-polymerization solution by selecting monomers able to recognize and assembly with more selectivity and affinity the template. This will allow for a selective template-functional monomer assembly and thus in an enhancement of the recognition properties. Further, this will allow for a much more rapid investigation of possible composition rather than the typical imprinting approaches [3].

Despite the importance, very few works have looked at the pre-polymerization complex in an attempt to optimize its selectivity, affinity and stability. Among those, some recent works emphasize this concept and propose alternative and smart strategies to address this issue.

Schrader group involves the use of hydrophilic copolymers that are not crosslinked upon interaction with the target protein (lysozyme) and thus the recognition is due entirely to the template induced fit. The entropic cost of freezing out conformational flexibility of the

protein is overcome by the maximization of favorable interactions between the chemical functionality in the monomers and the surface amino acids on the protein. Additionally, to provide a signaling functionality a fluorescent reporter (dansyl) is introduced in the system [69].

In another work reported by Min-Jie Guo, Assistant Recognition Polymer Chains (ARPCs) were introduced as additional functional monomers in the synthesis of a protein-imprinted polymer. In particular, the template protein was selectively assembled with ARPCs from their library, which consists of numerous limited length polymer chains with randomly distributed recognition and immobilizing sites. Subsequently, the selective assembly was adsorbed and immobilized by polymerization resulting in highly selective binding sites [70, 71, 72].

In a recent work, Takeuchi prepared thin films of protein-imprinted polymers using a semi-covalent approach. In particular, MIPs bearing peptide fragment-based binding sites were prepared by co-polymerization of the acrylated protein template with a newly synthesized co-monomer and crosslinker, followed by enzymatic decomposition of the grafted protein in the polymer matrix and creation of peptide fragment-based protein-binding site. To date, following the decomposition of the protein, co-monomer and crosslinker remain to function as binding sites within the imprinted cavity [73].

Pei-Chen Chou and co-workers developed a MIP selective for C-reactive protein (RCP) by mimicking the natural binding of CRP to its natural ligand phosphorylcholine (PC). They used as functional

monomer an analogue (phosphorylcoline derivative 4NPPC) of the naturally occurring ligand of the CRP (figure 10) [74].

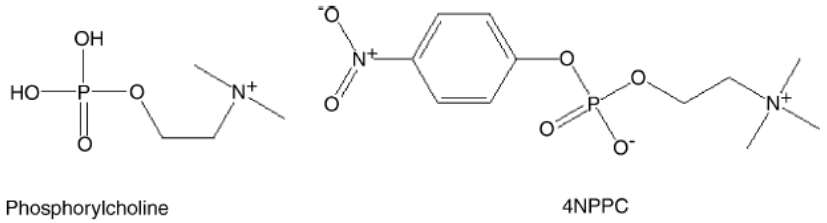

Figure 10. Comparative structure of phosphorylcholine and 4NPPC [74].

From the paucity of the literature, it seems clear that very few attempts have been made in the optimization of the pre-polymerization complex. However, the work of Takeuchi using peptide fragment-based binding sites and of Min-Jie Guo using ARPCs, emerge as the most promising strategies, emphasizing the crucial rule of choosing the right monomers.

1.3.7. Signaling MIPs functionality

In addition to the highly specific recognition abilities, the key step for future success of MIPs in a broader range of sensing applications is introducing a signaling functionality so that the binding event can be directly assessed [75]. In the last years, an increasing number of papers were emerging in this field and the strategies associated based on different techniques, including the development of new monomer molecules with responsive functionalities (such as environment-sensitive fluorescent probes), the conjugation of binding sites with transducers (molecular wires), and the utilization of induced conformational changes upon binding. Among optical techniques such as UV/Vis, IR spectroscopy, surface

plasmon resonance, chemiluminescence, refractive interference spectroscopy and Raman scattering, fluorescence is emerging as the most promising tool for studying MIPs due to its high sensitivity and simplicity [76]. In fact, fluorescence labeling can be used to probe the local environment obtaining a wide variety of information ranging from polymer structure and binding properties, to the transduction itself of the binding event [76, 77]. The fluorescent detection in MIPs can be achieved in different ways. In the easier case, the analyte is intrinsically fluorescent and give rise to an analytical signal upon binding to the MIP. However very few analytes allow direct detection and a labeling of the template is required prior the detection [78]. Additionally, in these cases the MIPs are only used for separation, the detection has to be carried out in a second, discontinuous step which is not ideal for sensor applications [75]. More frequently the analyte has no fluorescent property and the signaling functions have to be introduced [79]. Fluorescent-based MIPs are an attractive signaling method. Although the literature is scarce, even less for protein targets, quantum dots, noble metal nanoparticles, and fluorescent monomers are emerging as the most common fluorescent reporters [76]. In a recent work, Zhang synthesized a fluorescent MIP by coating quantum dots with an imprinted polymer for the specific recognition of cytochrome C [80]. In another work, Takeuchi prepared HSA-imprinted polymers using a dansyl-conjugated functional monomer designed to specifically interact with the target protein [81]. However, in these approaches the fluorescent reporter can be located outside the imprinting cavity or encapsulated into the

material, leading to high background fluorescence [82]. In order to reduce this shortcoming, Takeuchi proposed a novel strategy by introducing a fluorescent reporter into the molecularly imprinted cavity by a post-imprinting modification which enables to introduce the reporter molecule only at the position of the functional monomer located around the imprinted cavity created by the removal of the template protein [83]. Nevertheless, due to the presence of uncomplexed functional monomers in the pre-polymerization mix, the free functional monomers can be randomly located in the resulted polymer leading to an increase of fluorescence background and decrease of sensitivity. To enable a more sensitive and selective MIP, the same group modified the protocol preparing a MIP using a protein covalently conjugated to cleavable functional monomer that after template removal, allow for the introduction of the fluorophore only inside the cavity (Figure 11) [84]. Although this covalent imprinting approach provides more specific cavities, on the other hand the conjugation is complicated, time-consuming and could affect the protein conformation [85].

A new strategy called - Protein Imprinted Xerogels with Integrated Emission Sites - (PIXIES) reported by Tao relies upon sol-gel derived xerogels, molecular imprinting and the protein target itself to simultaneously create the site and assist in the selective installation of a luminescent reporter molecule directly within the imprinted site [86].

As emerge from the literature, there are several key challenges that one must overcome to develop a fluorescent-MIP sensor for the selective detection of a protein. First, one must synthesize a MIP

with affinity and selective recognition sites for the analyte. Second, one must accurately place the fluorescent reporter element in close proximity to the template site so as to effectively transducer the binding event, reducing the high fluorescent background noise and enhancing the sensitivity [86].

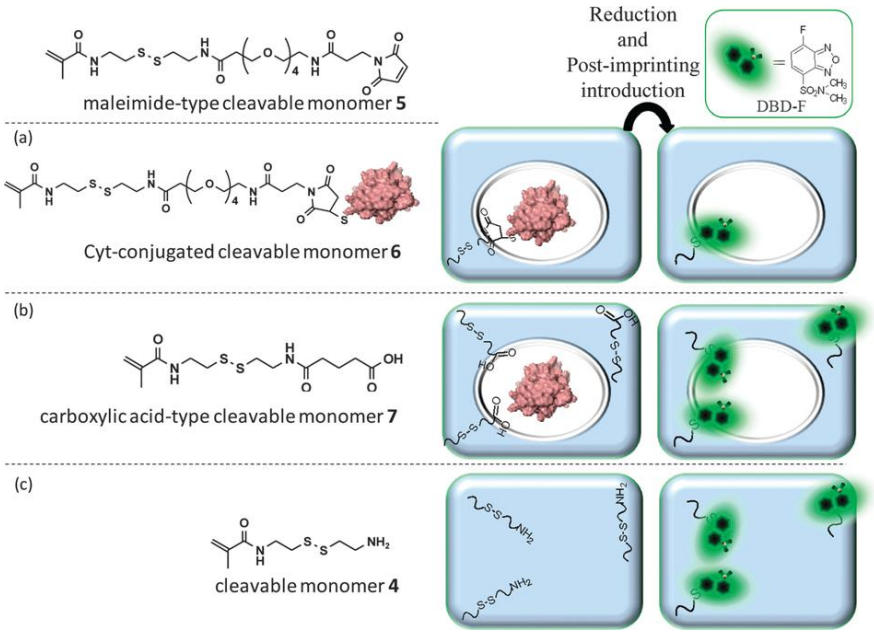

Figure 11. Schematic illustration of the preparation of MIPs along with post-imprinting treatment. (a) MIPs, (b) comp-MIPs, and (c) NIPs [84].

At this point, MIPs in which fluorescent functionalities are directly incorporated in the polymer are scarce and however, the quenching of a randomly located dye, lacking designated receptor sites, lead to a high fluorescence background and can only be employed for analytes which are potent quenchers. The covalent integration of a fluorescent probe monomer into MIPs emerges as the most promising strategy. However this, has only seldom been accomplished and especially examples showing directional

recognition at a designated binding site or fluorescence enhancement upon analyte binding are rare [75].

Chapter 2. Aim of research

The aim of this project is focused on the design and development of a novel synthetic material for the specific detection of a protein target. The material is based on a fluorescent molecularly imprinted polymer able to recognize the target and transduce the binding event into a measurable signal. The recognitive properties were addressed by incorporating an assistant-biomolecule into the imprinted cavity. The assistant-biomolecule was conjugated to an environment-sensitive fluorophore to provide the signal transduction function through the conversion of the binding event into a fluorescence change.

Chapter 3. Materials and methods

Acrylamide (Aam), Acrylic acid (AAc), Methylene bisacrylamide (MBA), Bovine Serum Albumin (BSA), Sodium chloride (NaCl), BSA-Fluorescein isothiocyanate conjugate (FITC-BSA), Lysozyme (LYS), Ovoalbumin (OVA), Fluorescein isothiocyanate (FITC), Disodium carbonate (Na_2CO_3), Potassium persulfate (KPS), N,N,N',N'-Tetramethylethylenediamine (TEMED) were purchased from Sigma-Aldrich (St. Louis, MO, USA). Phosphate buffer saline (PBS) was provided as tablets by MP Biomedicals and was always used at pH 7.4 0.01 M. Reagents for peptide synthesis (Fmoc-protected amino acids, resins, activation, and deprotection reagents) were from IRIS biotech. Solvents for peptide synthesis and HPLC analyses were from Sigma-Aldrich.

3.2. Target

3.2.1. Selection

An exhaustive analysis of the literature reveals that almost all reports employ a number of well defined model proteins as templates. Among these, Bovine Serum Albumin (BSA) is one of the most common model proteins. Serum albumin is a versatile carrier protein, and one of the most important blood proteins. Since this protein is so common in the blood and so easy to purify, resulting in relatively low cost preparation, it was one of the first proteins to be studied by scientists, when a generic protein is needed. Moreover, its structure has also been well-characterized.

For all these reasons, BSA has been selected as model protein for the work presented here.

3.3. Peptides

3.3.1. Selection

With the aim of develop a successful imprinted polymer, the formation of a monomer-template complex with multiple highly specific interactions is of crucial importance. An exhaustive selection of functional monomers prior to the imprinting procedure, results in a selective assembly of the template and thus in highly specific recognition sites. To address this issue, an extensive screening of molecules that selectively bind BSA template has been conducted. Among all the binders of the BSA taken from the literature, peptides have been evaluated as the most suitable binders for our purpose because of their exceptional affinity versus proteins, stability, ease of synthesis, purification and site-specific modification for further functionalities [21]. In particular, Dennis, identified a series of peptides (Serum Albumin peptides, SA-peptides) by phage display peptide libraries, having "DICLPRWGCLW" as the core sequence, that specifically bind albumin from multiple species with high affinity [87]. Further Dennis demonstrated the importance of the disulfide bridge in the recognition of albumins. Starting from the core sequence, for our purpose a series of site-specific modifications for tailor-made peptides has been actuated. First, in order to enhance the hydrosolubility of the peptide, four charged residues have been

added; in details, two glutamic acid residues each ones at both terminals, while at the C-terminal two aspartic acid residues. Second, the ability to be immobilized into the polymer matrix has been achieved by introducing at the C-terminal a modified aspartic acid residue bearing an allyl group. Additionally, a β-alanine has been introduced to space the allyl group from the core sequence. Third, in order to perform as a signaling fluorescent reporter a dansyl-lysine, spaced out two β-alanine to the peptide sequence, has been introduced at the N-terminal. The resulting peptide is named "SA-allyl-dansyl-peptide". Furthermore, a negative control denominated SA-allyl-dansyl-ctrl(-)peptide, in which most of the residues of the core sequence have been substituted with glycine residues, has been synthesized.

3.3.2. Synthesis

Single peptides were prepared by the solid phase method on a 75 μmol scale following the Fmoc strategy and using standard Fmoc-derivatized amino acids. Briefly, peptide synthesis was performed on a fully automated multichannel peptide synthesizer Biotage Syro Wave. Rink amide resin (substitution 0.71 mmol/g) was used as solid support. Activation of amino acids was achieved using HBTU-HOBt-DIPEA (1:1:2), whereas Fmoc deprotection was carried out using a 40% (v/v) piperidine solution in DMF. All couplings were performed for 20 min and deprotections for 15 min. Peptides were removed from the resin by treatment with a TFA:TIS:H_2O (90:5:5, v/v/v) mixture, then they were precipitated in cold diethylether and lyophilized. After purification step, single peptide was cyclized by formation of disulfide bridges. Briefly, a peptide was dissolved in

carbonate buffer at dilute solution (0.1 mg/mL) to favor intramolecular reactions; the pH was adjusted to 8.5 – 9.0 whilst stirring the solution at RT in presence of atmospheric oxygen for 24 h. The reaction was followed by HPLC. The cyclized peptides were purified by HPLC to remove any traces of sodium carbonate and lyophilized.

3.3.3. Characterization

3.3.3.1. HPLC

The purification and characterization of the peptides were performed by high performance liquid chromatography (HPLC). Single peptides were purified by preparative reversed-phase high performance liquid chromatography (RP-HPLC) using a Waters 2535 Quaternary Gradient Module, equipped with a 2489 UV/Visible detector and with an X-Bridge BEH300 preparative 10× 100 mm C8, 5µm column and applying a linear gradient from 5% to 60% over 25 min of 0.1% TFA/CH_3CN (solution B) in 0.1% TFA/water (solution A). Following, peptides purity and identity were confirmed by liquid chromatography mass-spectrometry (HPLC-MS) analyses, carried out on an Agilent 6530 Accurate-Mass Q-TOF LC/MS spectrometer. Zorbax RRHD Eclipse Plus C18 2.1 x 50 mm, 1.8 µm columns were used for these analyses.

3.3.3.2. Binding parameters - ITC

The binding parameters between SA-peptides and BSA were obtained by Isothermal Titration Calorimetry (ITC), (nano-ITC low-

volume calorimeter, TA Instruments). Single SA-peptide dissolved in PBS (1 mM) was loaded in injection syringe and titrated into a BSA solution in PBS (0.1 mM). The stepwise experiments were conducted with 25 injection of 2 μL of SA-peptide with 200 s intervals. These results have been corrected by subtraction of appropriate blank experiments to account for the heats associated with mixing and dilution reactions; this blank experiment was performed by injections of SA-peptide solution into the cell containing PBS alone. The heat released upon interaction between SA-peptide and BSA is monitored over time so that each peak represents a heat change associated with the injection of a small volume of samples into the ITC reaction cell. As successive amounts of the ligands are titrated, the quantity of heat adsorbed or released is in proportion to the amount of binding. The binding curve is then obtained from a plot of the heats from each injection against the ratio of ligand and binding partner. The resulting data, after appropriate corrections, were fitted to an independent and equivalent binding-site model with NanoAnalyze software.

3.3.3.3. Binding parameters - SPR

The binding parameters were also confirmed by Surface Plasmon Resonance (SPR), using a fully automated SensiQ Pioneer optical biosensor. BSA was immobilized in 10 mM acetate buffer pH 3.7 (flow rate 5 μL/min, time injection 7 min) on a SensiQ COOH5 sensor chip, using EDC/NHS chemistry. Residual reactive groups were deactivated by treatment with 1 M ethanolamine hydrochloride, pH 8.5. References channels were prepared simply activating with EDC/NHS and deactivating with ethanolamine.

Affinities SPR experiments were carried out injecting SA-peptide at different concentrations (injections of 90 μL at a flow rate of 20 μL/min). The bound peptide was allowed to dissociate for 5 min before matrix regeneration using 10 mM NaOH. The signal from an injection passing over the immobilized protein, was subtracted from that of the reference channel to generate sensogram of the amount of peptide bound as a function of time. For equilibrium analysis, the response at equilibrium was plotted against the analyte concentration and fit to a 1:1 binding isotherm using the Qdat and GraphPad analysis software.

3.3.3.4. Fluorescence properties

To evaluate the spectral properties of fluorescent SA-peptides, fluorescence emission spectra of free form and complexed form with BSA were collected in a quartz cell using a spectrofluorometer (FluoroMax-4 Horiba Scientific). The spectra were recorded in PBS (pH 7.4 0.01 M) by exciting at 340 nm and collecting emission between 400 and 630 nm with 5 nm bandpass. A single fluorescent SA-peptide (1 μM) was titrated by dropping 0.8 uL aliquots of BSA solution (100 μM). Then, emission spectra of complexed peptides were compared with the free forms. In addition, in order to ensure that fluorescence was not derived from dilution of BSA in buffer, fluorescence spectra of BSA solutions at different concentration were recorded.

3.4. Molecularly imprinted polymers

3.4.1. Synthesis

3.4.1.1. Imprinting design

As mentioned in the chapter 1, acrylamide-based polymers possess a series of advantages that make them promising materials for imprinting proteins. As result, Aam has been chosen as polymer matrix for the imprinting of BSA. The polymer network consisted of two functional monomers (Aam and AAc) and a crosslinking monomer (MBA). The relative amounts of the monomers have been modulated according to the key parameter: T% and C%. To date, T% has been fixed to 15 while C% to 10. In addition, taking in account the reactivity ratio of the monomers, the ratio between Aam and AAc (expressed in %w/v) has been fixed to Aam/AAc 2:1. The M/T molar ratio has been fixed to 10000:1 in order to maximize the specific interactions between the protein and the monomers. The SA-allyl-peptides were added in 1:1 molar ratio with the BSA, as previously proved by ITC and SPR analysis. Polymerization was initiated with KPS (0.6 %w/v monomers) to generate free radicals and was catalyzed by TEMED (0.8 %w/v monomers). PBS 0.01 M at pH 7.4 has been chosen as solvent for the polymerization to maintain all imprinting reagents into physiological conditions. Finally, bulk approach has been selected as the most useful approach to our scope.

3.4.1.2. Imprinting procedure

The synthesis of MIP-SA-allyl-peptide using SA-allyl-peptide as assistant-monomer, proceeded via a multistep procedure. Firstly,

SA-allyl-peptide was added to a BSA solution in a vial and incubated at RT, under gentle stirring for 30 min for selective assembling. In a vessel, Aam, AAc and MBA were mixed and pH adjusted to 7.0 with NaOH 10 M. Then, the mix of monomers was added to BSA-SA-allyl-peptide complex solution and incubated for allowing the assembling of functional monomers with the complex (30 min under gentle stirring). After purged the solution with N_2 for 3 min, KPS and TEMED were added to the solution and the radical free polymerization was initiated and continued for 30 min at RT under vigorous magnetic stirring and continuous nitrogen stream. Once terminated the polymerization, the monolithic gel was collected in a beaker, added with 90 mL PBS and undergo to a homogenizer cycle for 15 min to produce sub-150 μm particles. The resultant microparticles were transferred in 50 mL conical tubes, collected by centrifugation at 4500 rpm for 10 min and washed repeatedly to remove adsorbed oligomers and unreacted monomers. In particular, the polymers were washed with four rinses of PBS followed by four rinses with NaOH 1M/PBS and four rinses more in water to remove any traces of PBS and NaOH. Finally, the micro-particles were freeze-dried and stored at 4°C for further uses. The same procedure was used for the synthesis of MIP-SA-allyl-dasnyl-peptide and MIP-SA-allyl-ctrl(-)peptide. Control polymers (non-imprinted polymers, NIPs) under exactly the same conditions but in absence of protein, were also prepared.

3.4.2. Characterization

3.4.2.1. Microparticle size

The size of the polymers was estimated by laser diffraction method (Mastersizer 2000, Malvern Instruments). The dried microparticles, dispersed in PBS 0.01 M, were measured after 90 s of sonication to prevent aggregation before measurement.

3.4.2.2. Chemical composition

The chemical characterization of the polymers was performed by Fourier Transform Infrared Spectroscopy (FT-IR) using a Nicolet 6700 FT-IR spectrometer (Thermo Scientific). The FT-IR spectra of dried polymers were recorded with 256 scans in the range of 4000-600 cm^{-1}.

3.4.2.3. Template removal

To validate the washing procedures, samples from each rinse were analyzed for residual BSA via UV spectroscopy at 280 nm. Briefly, after the addition of a known volume of a desired wash solution, the sample were placed on a rotating mixer for 20 min to allow adequate time for diffusion, and centrifuged for 10 min (4500 rpm). Then 1 ml sample was pipetted out of the supernatant for UV analysis, and the residual supernatant was recorded and decanted. The time for diffusion was chosen by taking in account the diffusion coefficient of BSA in water at 20°C ($5.9 \cdot 10^{-7}$ cm^2/sec) [88] and the microparticles diameter previously determined. The amount of BSA removed at step *i* was calculated by equation:

$$M_i = (V * C)_{MIP} - (V * C)_{NIP}$$

Where M is the BSA mass removed in step *i*, V is the volume of supernatant decanted in step *i* and C is the protein concentration determined from absorbance measurement using Lambert-Beer equation. The control is subtracted out because unreacted monomers can absorb at this wavelength. The volume decanted multiplied by the concentration of protein will give an the mass of BSA removed. The mass removed in each step was added together to yield a total mass removed, which was then compared to the amount of BSA added in the MIP synthesis.

3.4.2.4. Affinity binding studies

Affinity binding studies were performed by confocal fluorescence laser-scanning microscopy analysis by using a fluorescent BSA conjugate (albumin fluorescein isothiocyanate conjugate, FITC-BSA) to visualize the adsorption on the polymer. Images of polymers were collected by a CLSM Leica TCS SP5, using argon laser line 488 nm, objective 40.0x1.10 water, scan speed 400 Hz, λem range 500-550 nm. Five images were collected for each sample. By analyzing fluorescent intensity values from polymer microparticles of similar size, quantitative analysis of FITC-BSA amount bound to the network was obtained. The experimental parameters (such as excitation time, objective and field of view) were precisely matched for an accurate quantitative analysis. All captured images were analyzed with Image-J software.

3.4.2.4.1. Equilibrium binding studies

For the equilibrium binding studies, a known amount of freeze-dried polymer (5 mg) of a specific formulation was dissolved in 0.5 mL of PBS (0.01 M pH 7.4,) and placed on a rotating mixer for 20 min to allow swelling. Then, 0.5 mL of FITC-BSA solutions at different concentrations was added to the polymer solutions to give final FITC-BSA concentrations (0.01; 0.03; 0.075; 0.15; 0.75; 1.5; 2.25 μM) and a final particles concentration of 5 mg/mL. Samples were placed in a rotating mixer and allow for equilibrating for 3 hours. The time for equilibrium was predetermined by separate kinetic binding studies. Once reached the equilibrium, 0.02 mL of the polymer solution was collected and analyzed to the microscope as described is section 3.4.2.4. The dissociation constants were obtained by fitting the average fluorescence values from each polymer with a non-linear specific-binding model using GraphPad software.

3.4.2.4.2. Kinetic binding studies

For kinetic binding studies, a known amount of freeze-dried polymer (5 mg) of a specific formulation was dissolved in 0.5 mL of PBS (0.01 M, pH 7.4) and placed on a rotating mixer for 20 min to allow swelling. Then, 0.5 mL of FITC-BSA solution at different concentrations was added to the polymer solutions to give final FITC-BSA concentrations (0.15, 0.75, 1.5 μM) and a final particles concentration (5 mg/mL). At varying time points (5, 10, 20, 60, 120 min), an aliquot (0.02 mL) of the polymer solution was collected and analyzed to the microscope as described in section 3.4.2.4. The

dissociation constants were obtained by fitting the average fluorescence intensity from each polymer at each time point with a non-linear specific-binding model using GraphPad software.

3.4.2.5. Competitive binding studies

Competitive binding studies were performed to evaluate the selectivity of MIPs. Lysozyme (LYS) (MW ~14.5 kDa, pI 11.3) and Ovalbumin (OVA) (MW ~44.3 kDa, pI 4.5) were chosen as competitor proteins because of their different size and charge to those of BSA (MW~66.5 kDa, pI 4.9). BSA was used as competitor control protein. Briefly, a known amount of freeze-dried polymer (5 mg) of a specific formulation was dissolved in 0.2 mL of PBS (0.01 M, pH 7.4) and then placed on a rotating mixer for 20 min to allow swelling. Then, 0.4 mL of FITC-BSA solution (0.075 μM) was added to 0.4 ml of competitor protein solutions at different concentrations to give final solutions of protein mixtures with different FITC-BSA:competitor protein molar ratio (1:0, 1:100, 1:300). After, 0.8 mL of these protein mixture solutions was added to the polymer solution to give a final volume of 1 mL. The samples were placed in a rotating mixer and allow for equilibrating for 3 hours. Once reached the equilibrium, an aliquot (0.02 mL) of the polymer solution was collected and analyzed to the microscope as described in section 3.4.2.4.

3.4.2.6. Transduction signaling studies

In order to evaluate the ability of MIP-SA-allyl-peptide to transducer the binding event into a quantifiable signal, SA-allyl-

dansyl-peptide has been introduced into the polymer network. The resultant MIP-SA-allyl-dansyl-peptide has been studied by using multiphoton laser scanning microscopy. This technique allows for a study of binding event and direct observation of the fluorescence changes upon adsorption of BSA within the polymer. The equilibrium binding studies were performed as described in section 3.4.2.5 using MIP-SA-ally-dansyl-peptides and the control polymer (MIP-SA-ally-dansyl-ctrl(-)peptide) as polymers and BSA (no labelled) to visualize the binding. Furthermore, differently from equilibrium studies in section 3.4.2.4, as BSA is used as analyte, no dilution of the polymer suspension was required. Images of polymers were collected by a CLSM Leica TCS MP-SP5, using a multiphoton laser λexc 700 nm, objective 25.0x1.10 water, scan speed 400 Hz, λem range 490-510 nm. All the steps following the collect of the images were performed as described in section 3.4.2.4.

Chapter 4. Results and discussion

4.1. Peptides

4.1.1. Synthesis

Four different SA-peptides were synthesized by the solid phase method following the Fmoc strategy (table 7).

SA-PEPTIDES
SA-peptide (36 % yield) E**DI<u>C</u>LPRWG<u>C</u>LW**EDD
SA-allyl-peptide (14 % yield) E**DI<u>C</u>LPRWG<u>C</u>LW**EDD-βA-D(Oall)
SA-allyl-dansyl-peptide (7.7 % yield) K-dansyl-βAβA-E**DI<u>C</u>LPRWG<u>C</u>LW**EDD-βA-D(Oall)
SA-allyl-dansyl-ctrl(-)peptide (12.1 % yield) K-dansyl-βAβA-EGG**<u>C</u>**GG**R**G**G<u>C</u>**GGEDD-βA-D(Oall)

Table 7. Denomination, sequence and yield of peptides. Single-letter amino acid code is used for the peptide sequences. Amino acids in bold indicate amino acids of the core sequence while the underlined ones involved in the disulphide bridge.

4.1.2. Characterization

4.1.2.1. HPLC

The purification and characterization of the peptides were performed by RP-HPLC. Following, peptides purity and identity were confirmed by HPLC-MS analyses. The overall results of peptide synthesis and characterization are reported in appendix A. The analysis of crude, purified and cyclized peptide were reported for each peptide. To date, for each analysis the total ion chromatogram (TIC) and the corresponding signal from the diode

array detector (DAD) at 280 nm are reported. Then, the major peak in the TIC and in the DAD was extracted, providing the UV spectra and the electrospray ionized mass spectra (ESI) of a single peptide. The UV spectra show intense peaks at 220 and 280 nm that are indicative of the presence of a peptide. The mass spectra show the fragment ion peaks that allow for the identification of a peptide by attributing the peaks to a specific pattern of peptide fragmentation. The results showed that the four SA-peptides were successfully synthesized, with the expected amino acid compositions and with different yields (table 7).

4.1.2.2. Binding parameters - ITC

The binding properties of SA-peptides were obtained by ITC analysis. Furthermore, in order to asses that the introduced modifications did not alter significantly the binding properties, ITC analysis of SA-allyl-peptide was also carried out. The figure 12 illustrates ITC data of SA-peptide and SA-allyl-peptide.

By titrating aliquots of SA-peptide into BSA solution, the ITC titration peaks demonstrated that the binding between SA-peptide and BSA is an exothermic reaction. These raw data can be fitted according to an independent and equivalent binding-site model which provided the thermodynamic parameters (table 8). These parameters provided a series of information about the binding of SA-peptide to BSA. First, the stoichiometry of binding (n) is 1.068, indicating that one molecule of SA-peptide binds to one molecule of BSA. Second, the dissociation constant (K_D) is 21.66 μM, in the same order of magnitude to that estimates by Dennis [87] for

peptide SA15 (K_D 0.878 μM). Third, the binding is accomplished by favorable entropy (TΔS) indicating that the binding is entropically driven.

This indicates that SA-peptide has been successfully synthesized, and it is able to bind BSA with the same affinity to that reported in literature. Similar thermodynamic parameters have been obtained for SA-allyl-peptide demonstrating that the modifications introduced to the peptide sequence do not alter significantly the structure and thus the binding properties of the peptide.

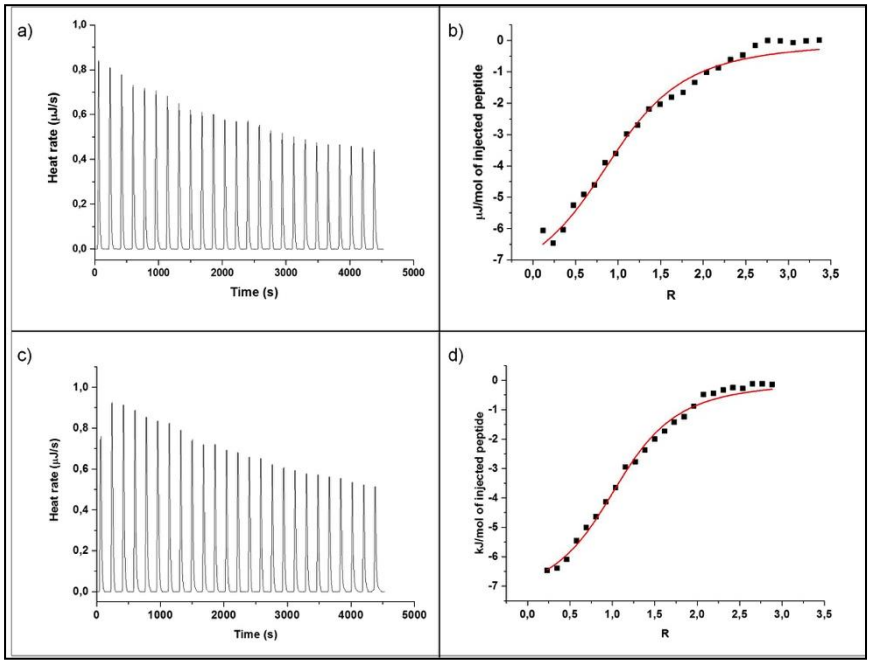

Figure 12. Raw (a,c) and integrated (b,d) data of SA-peptide and SA-allyl-peptide in the upper and lower part of the figure, respectively.

	Ka (M^{-1})	**n**	**ΔH (kJ/mol)**	**K_D (μM)**	**TΔS (kJ/mol)**
SA-peptide	4.616E4	1.068	-7.955	21.66	18.6
SA-allyl-peptide	7.590E7	1.125	-7.487	13.18	20.3

Table 8. Table resuming thermodynamic signature of SA-peptide and SA-allyl-peptide binding to BSA. Abbreviations: n, stoichiometry of interaction; Ka, association constant; ΔH, enthalpy; K_D, dissociation constant; TΔS, entropy.

4.1.2.3. Binding parameters - SPR

In order to further confirm the binding properties of SA-peptide, a Surface Plasmon Resonance analysis was carried out.

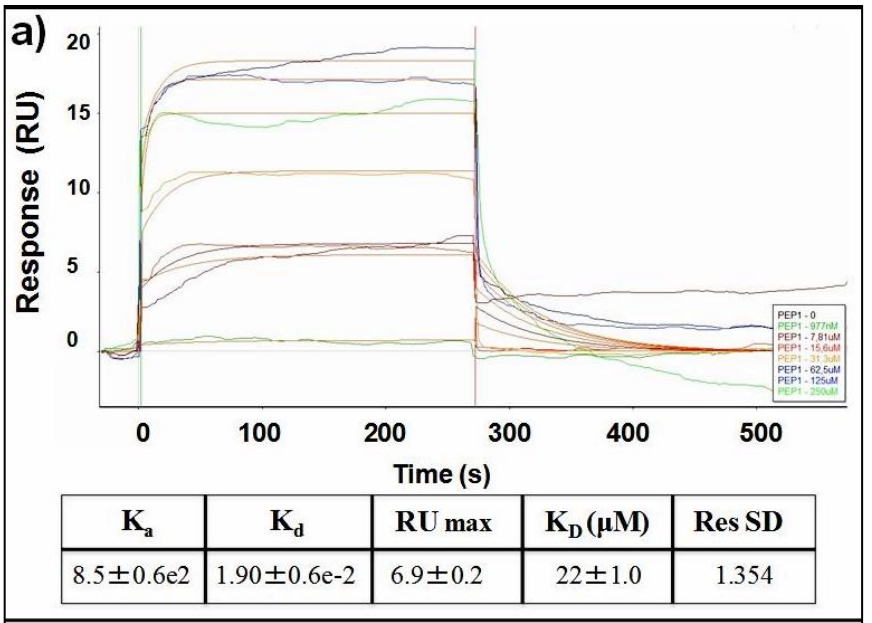

K_a	K_d	RU max	K_D (μM)	Res SD
8.5±0.6e2	1.90±0.6e-2	6.9±0.2	22±1.0	1.354

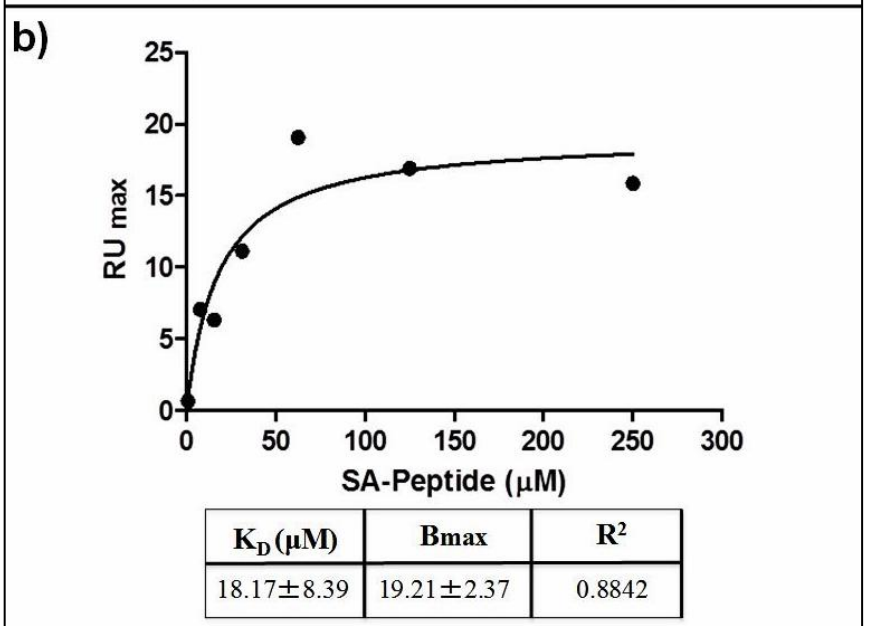

K_D (μM)	Bmax	R^2
18.17±8.39	19.21±2.37	0.8842

Figure 13. SPR data of SA-peptide, a) overlay of sensograms relative to the binding of SA-peptide to immobilized BSA, b) plot of RUmax from each experiment versus SA-peptide concentration.

Direct binding between the protein and SA-peptide was performed by injecting peptide solutions at increasing concentrations. As shown in the sensogram (figure 13a), SA-peptide binds BSA in a dose-response manner with a dissociation constant (K_D) of 22 μM. By plotting RU max values from each binding experiment as a function of BSA concentrations (figure 13b), a K_D value of 18.17 μM was obtained. This indicates that both K_D are in good agreement with that reported by Dennis [87] for SA15 (K_D 0.878 μM) and supports the view that SA-peptide was successfully synthesized with affinity comparable to the literature.

4.1.2.4. Fluorescence properties

In order to corroborate the affinity values evaluated through SPR, using a completely solution binding assay, a fluorescent titration of fluorescent SA-peptides with BSA was performed. The peptides were labelled by introducing a fluorescent-sensitive fluorophore (Lysine-dansyl) at their N-termini and fluorescence emission at ~500 nm was measured. In details, SA-allyl-dansyl-peptide and negative control peptide (SA-allyl-dansyl-ctrl(-)peptide) were titrated with BSA to evaluate the signaling function when bound to BSA. With the addition of BSA, SA-allyl-dansyl-peptide exhibits large changes in fluorescence (figure 14a).

To date, the binding of SA-allyl-dansyl-peptide to BSA results in about 9.6-fold increase in fluorescence intensity (F.I.) and 40 nm blue shift of the emission maximum (λmax). Notably, when BSA is added in molar excess, the emission trend of SA-allyl-dansyl-peptide did not change and the saturation was reached.

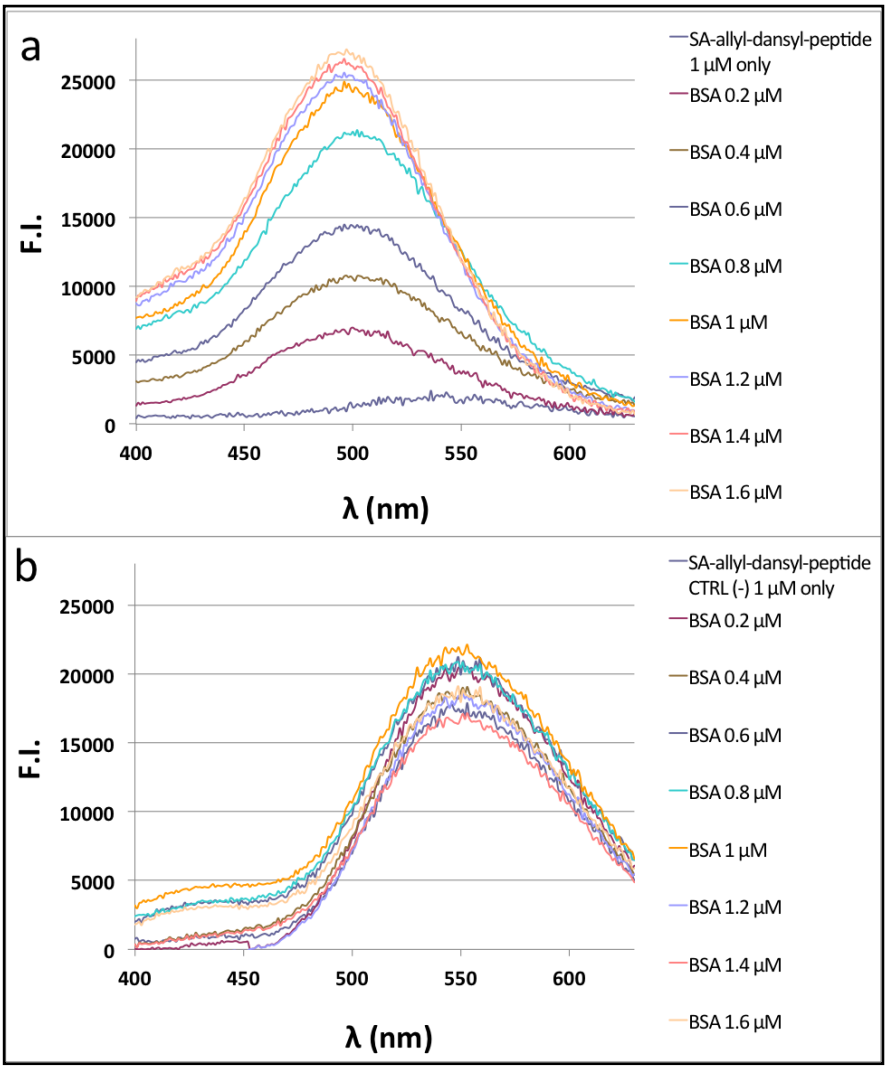

Figure 14. Fluorescence emission spectra of (a) SA-ally-dansyl-peptide and (b) SA-allyl-dansyl-ctrl(-)peptide upon increasing concentrations of BSA.

This is in accordance with ITC and SPR results which provided equimolar interaction between BSA and SA-peptide. Indeed, for SA-allyl-dansyl-ctrl(-)peptide the fluorescence intensity changes were smaller and emission λmax was not appreciably changed (figure 14b). Finally, fluorescence spectra of BSA at different concentrations show a λmax emission at 425 nm, outside the

emission range of dansyl (450-550 nm) (data not shown). Table 9 resumes the fluorescence properties of SA-allyl-dansyl-peptide and SA-allyl-dansyl-ctrl(-)peptide, including BSA.

Peptide	complex/ free form	λmax (nm)	F.I. at 500 nm	fold-increase F.I.	shift (nm)
SA-allyl-dansyl-peptide	free	540	2300	~9.6	40
	complex	500	22100		
SA-allyl-dansyl-ctrl(-)peptide	free	550	18000	~1.2	0
	complex	550	21900		
BSA	free	425	5300	~1.6	0
		425	8600		

Table 9. Fluorescence properties of SA-ally-dansyl-peptide and of SA-allyl-dansyl-ctrl(-)peptide in free form and bound to BSA. BSA fluorescence properties are also reported.

By fitting the relative fluorescence emission intensity ($\Delta F/F_0$) of each peptide with a binding isotherm model, a K_D for SA-allyl-dansyl-peptide can be obtained. To date, ΔF was calculated using the equation ($F-F_0$), where F_0 and F are the fluorescence intensities before and after the addition of BSA, respectively (figure 15). The K_D of SA-allyl-ctrl(-)peptide was not shown because the binding model does not fit the data. This because $\Delta F/F_0$ values obtained for SA-allyl-ctrl(-)peptide did not follow a dose-response behaviour. The results indicate that the fluorescence changes are due to the binding of SA-allyl-dansyl-peptide to BSA, with a K_D comparable with those reported in literature [87] and obtained by ITC and SPR experiments.

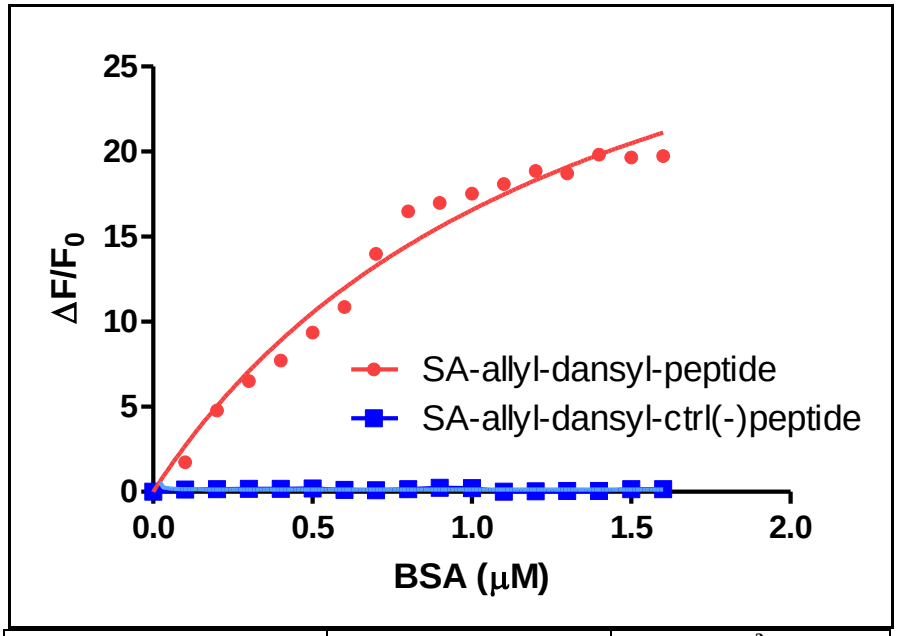

	K_D	R^2
SA-allyl-dansyl-peptide	1.351 ± 0.2556	0.9779

Figure 15. Fitting curves of SA-allyl-peptide and SA-allyl-ctrl(-)peptide in the upper part of the figure; table with dissociation constant of SA-allyl-peptide in the lower part of the figure.

Dansyl is an environment-sensitive fluorophore very sensitive to the polarity of the medium, with high fluorescence in low polarity environment [89]. As SA-allyl-dansyl-peptide binds BSA, the binding causes the inclusion of the peptide into a hydrophobic pocket in the protein. That inclusion results in a significant change in the microenvironment of dansyl upon binding to the protein, and corresponding changes of the fluorescence emission properties. Both fold-increase and shift of λmax are comparable with those reported in literature [43]. Differently, SA-allyl-dansyl-ctrl(-)peptide does not have affinity for BSA and thus no significant fluorescence emission changes are observed.

4.2. Molecularly imprinted polymers

4.2.1. Synthesis

4.2.1.1. Imprinting design

The optimization of the imprinting procedure has lead to establish the composition of the polymerization mixture. Figure 16 illustrates the chemical structures of the reagents, while the table 10 reports the composition of the reagents.

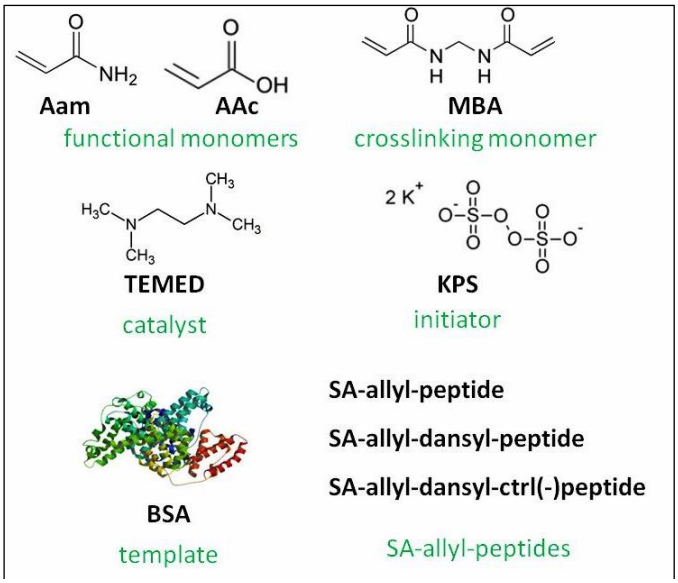

Figure 16. Chemical structure of reagents of the imprinting procedure. For the chemical structures of peptides see table 7.

REAGENT	%w/v
Aam	9
AAc	4.5
MBA	1.5
BSA	1.32
SA-allyl-peptide/ SA-allyl-dansyl-peptide/ SA-allyl-dansyl-ctrl(-)peptide	0.0412 0.0512 0.0408
KPS	0.32
TEMED	0.18

Table 10. Composition of reagents of the imprinting procedure.

4.2.1.2. Imprinting procedure

The synthesis of the molecularly imprinted polymers proceeded via a multistep process (figure 17). Four different kinds of imprinted polymers and corresponding control polymers (non-imprinted polymers) were prepared (table 11). To date, the preparations denoted as (b) contain SA-allyl-peptide as assistant-peptide, those denoted as (c) and (d) contain SA-allyl-dansyl-peptide and SA-allyl-dansyl-ctrl(-)peptide, respectively.

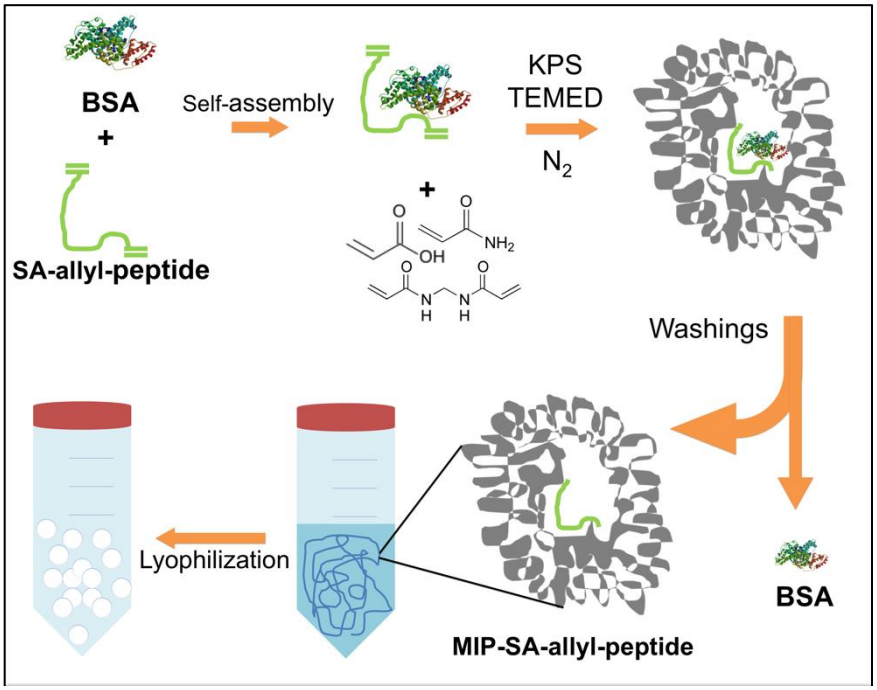

Figure 17. Schematic representation of imprinting procedure of MIP-SA-allyl-peptide.

	MIPs	NIPs
(a)	MIP	NIP
(b)	MIP-SA-allyl-peptide	NIP-SA-allyl-peptide
(c)	MIP-SA-allyl-dansyl-peptide	NIP-SA-allyl-dansyl-peptide
(d)	MIP-SA-allyl-dansyl-ctrl(-) peptide	NIP-SA-allyl-dansyl-ctrl(-)peptide

Table 11. MIPs and NIPs preparations.

4.2.2. Characterization

4.2.2.1. Microparticle size

The size of the polymer was estimated by a light diffraction technique. As the studies were conducted in PBS, the resulting polymer size was related to its relaxed state when the polymer is completely swollen. Polymer size is one of the most important characteristics of an imprinted polymer because it affects the mass transport properties of the template into the polymer matrix [90]. In order to obtain a control over particles size of the imprinted polymer and to achieve a sub-150 μm particle size [91], effect of different times of homogenizer on the polymer size was investigated.

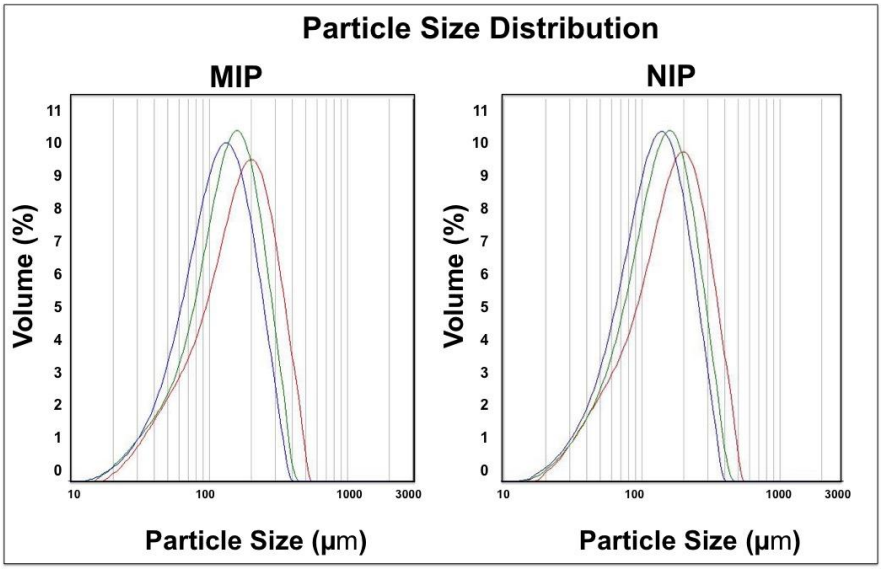

Figure 18. Particle size distribution of MIPs and NIPs at different time of homogenizer (in red 15, in green 10 and in blu 15 min).

The studies shown that the particle size of MIPs and NIPs decreases from 182.07 μm to 131.50 μm and from 181.10 to 135.73 μm with

the increase of time of homogenizer from 5 to 15 min, respectively (figure 18). However, the particle size distributions are relatively wide both for MIPs and NIPs.

These results demonstrate first, that the particles size is not affected by the presence of the protein as both preparations shown comparable particle size distributions over the entire cycles of homogenizer. Second, a cycle of 15 min of homogenizer is required to produce the desired sub-150 μm particles. However, the wide particle size distribution can affect subsequent template binding as different size results in different mass transport properties. Table 12 reports the particle size distribution expressed as mean volume %.

Sample	Time of homogenizer (min)		
	5	10	15
MIP	182.07	149.62	131.50
NIP	181.10	151.92	135.73

Table 12. Particle size distribution of MIP and NIP at different time of homogenizer.

4.2.2.2. Chemical composition

The chemical characterization of the polymers was performed by FT-IR. As shown in figure 19, the major peaks fall at the same frequency for all polymers and thus the spectra are nearly completely overlapped. This suggest, as expected, that all polymer preparations are equal in composition except for the presence of SA-allyl-peptide in MIP-SA-allyl-peptide and NIP-SA-allyl-peptide. However, the presence of the peptide in the polymer is not evaluable because its characteristic amide bonds peaks are hidden by the same peaks of acrylamide which is predominant. In fact, FT-IR spectra show characteristics adsorption bands related to the C(α)-

NH group which confirm the existence of amide bonds [92]. These bands are assigned as follow: a broad absorption band at 3400 cm^{-1} from the N-H asymmetric stretching vibration and two additional strong bands at 1661 cm^{-1} and 1557 cm^{-1} are assigned to the amide I (C=O stretching) and amide II (N-H bending) vibration, respectively. Further, FT-IR spectra show a characteristic peak at 1404 cm^{-1} that can be assigned to the symmetric stretching of COO^- of the acrylic acid. However, the spectra lack of the asymmetric stretching of COO- at 1550 cm^{-1} that is hidden by the strong peak of amide II. The FT-IR spectra results confirm that both Aam and AAc monomers has been successfully polymerized into the polymer network.

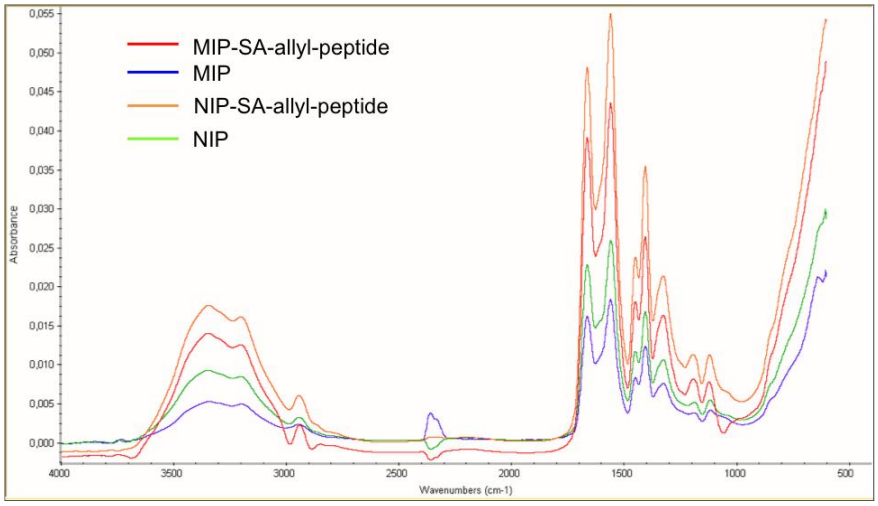

Figure 19. FT-IR spectra of polymer preparations.

4.2.2.3. Template removal

The study of the efficiency of template removal was carry out by UV analysis. The figure 20 illustrates an example of UV absorption

spectra of BSA with a peak at 279 nm indicative of the presence of the protein.

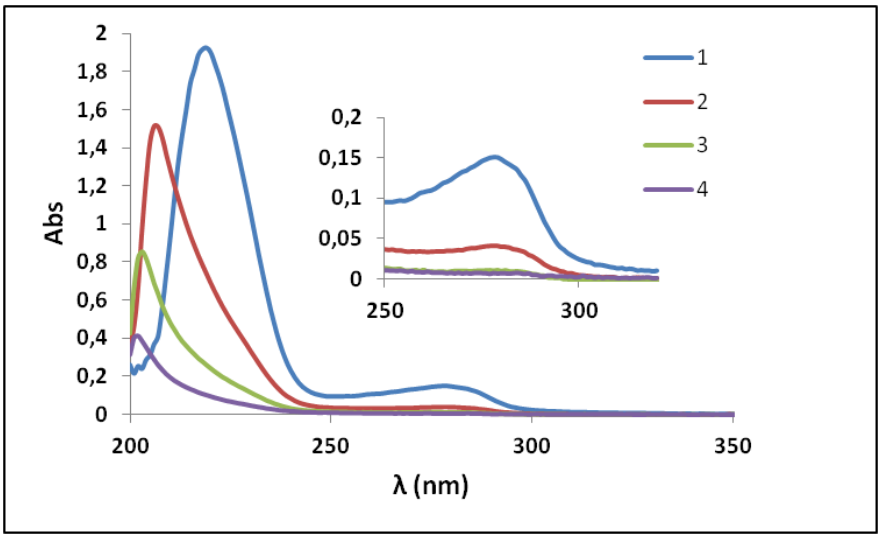

Figure 20. Example of UV-spectra of MIP supernatant relative to the four rinses in PBS. A UV-spectra magnification between 250 and 320 nm is also reported.

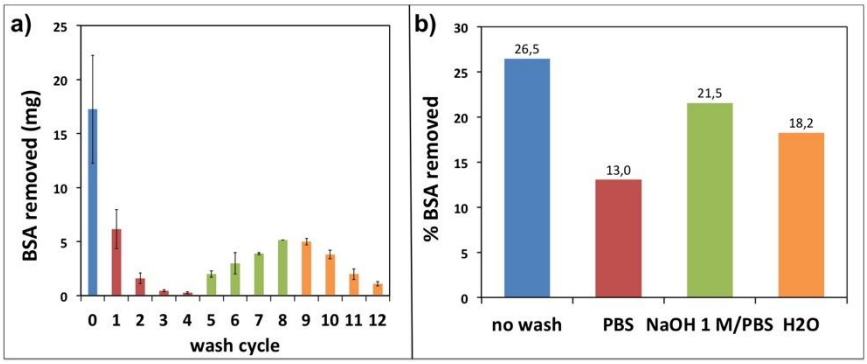

Figure 21. Histograms reporting a) mass of BSA removed at each wash cycle and b) % BSA removed with each washing solution.

The majority of BSA (17.2 mg) was removed without any washing, just homogenizing the polymer resulting in a crushing of the bulk polymer and thus a massive release of BSA (figure 21a). The first rinse in water yields to another quantitative release of BSA (6.1

mg). The subsequent rinses in NaOH 1 M/PBS produce an increasing release of BSA from the first to the fourth wash cycle. Finally, transferring the polymer in water, results in a progressive decrease of BSA release. The figure 21b resumes the % of BSA removed with each washing solution respect to the amount of BSA added in the synthesis. The trend was attributed to different grades of swelling of the polymer in each washing solution, leading different amounts of BSA removed. To date, the amount of BSA removed in NaOH 1 M/ PBS makes for 21.5 %, concluding that the polymer undergoes to an extensive swelling that enhances the mesh size and produces a greater BSA release. Summing the amount of BSA removed with each washing solution it is possible to estimate ~79.3 % as the total amount of BSA removed. These data prove an effective method in removing BSA at comparable levels to literature (~70-90 %) [93], minimizing swelling of the network and thus preserving the integrity of recognition sites.

4.2.2.4. Affinity binding studies

4.2.2.4.1. Equilibrium binding studies

In order to evaluate the adsorption properties of MIPs, equilibrium binding studies were performed. Equilibrium binding studies were performed by fluorescence microscopy that allows for a micro-scale observation of binding and direct imaging of the uptake of the fluorescent BSA conjugate within the polymer [94, 95]. Among the binding parameters, the maximum amount of protein that can be recognized at equilibrium is important in identifying the difference between imprinted and non-imprinted polymers.

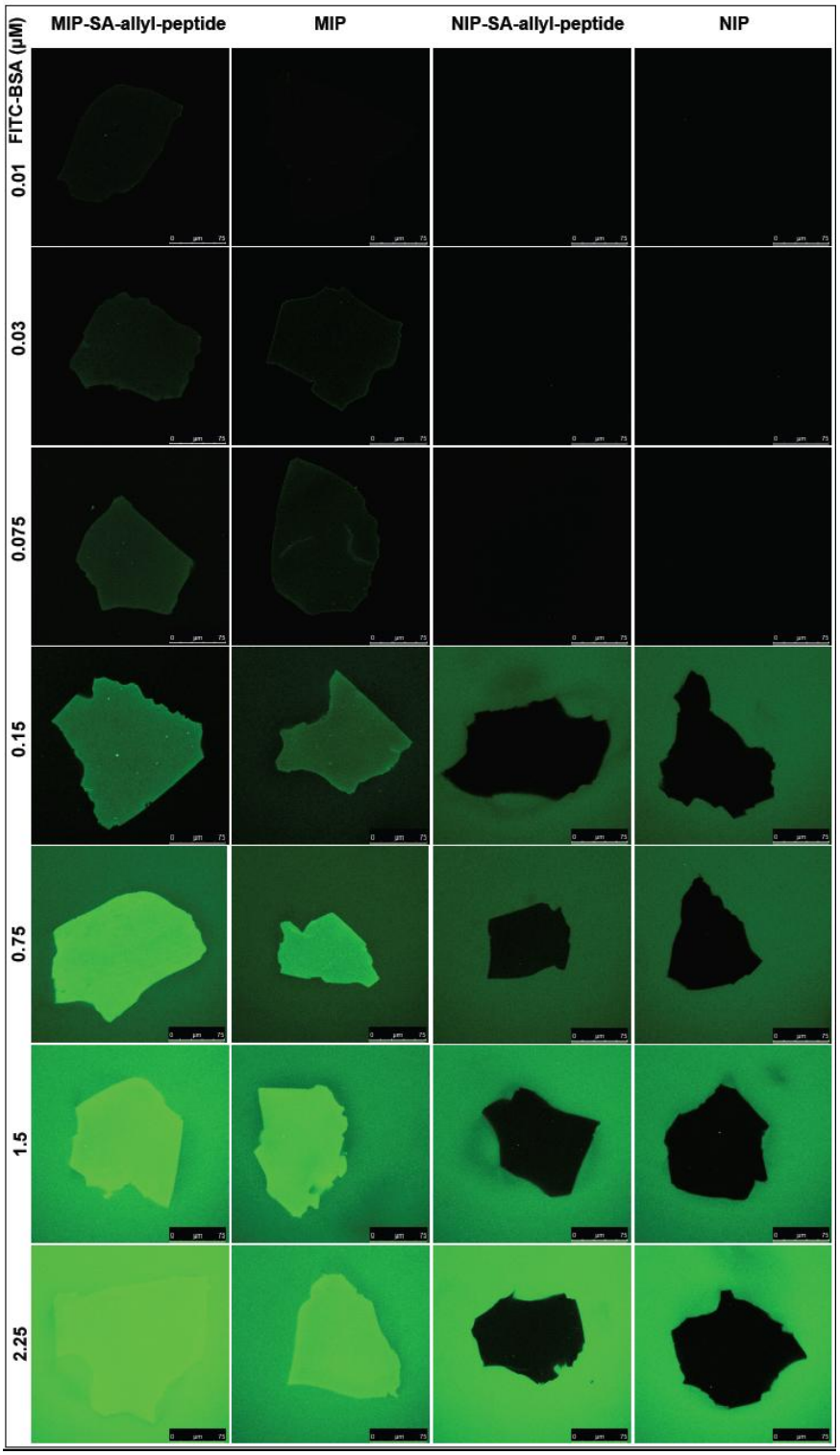
MIP-SA-allyl-peptide
MIP
NIP-SA-allyl-peptide
NIP
FITC-BSA (μM)
0.01
0.03
0.075
0.15
0.75
1.5
2.25

Figure 22. Fluorescence microscopy images of single microparticle of MIP-SA-allyl-peptide, MIP, NIP-SA-allyl-peptide and NIP added to varying FITC-BSA concentrations. MIP-SA-allyl-peptide shows higher fluorescence intensity due to a higher affinity for the fluorescent conjugate of BSA.

By analyzing fluorescence intensity of polymer microparticles of comparable size, a histogram of intensity values was obtained, which provided a quantitative analysis of template amount bound to the network. In figure 22 were shown the fluorescence microscopy images, while in figure 23 was shown the histogram of fluorescence intensity values obtained from MIP and NIP.

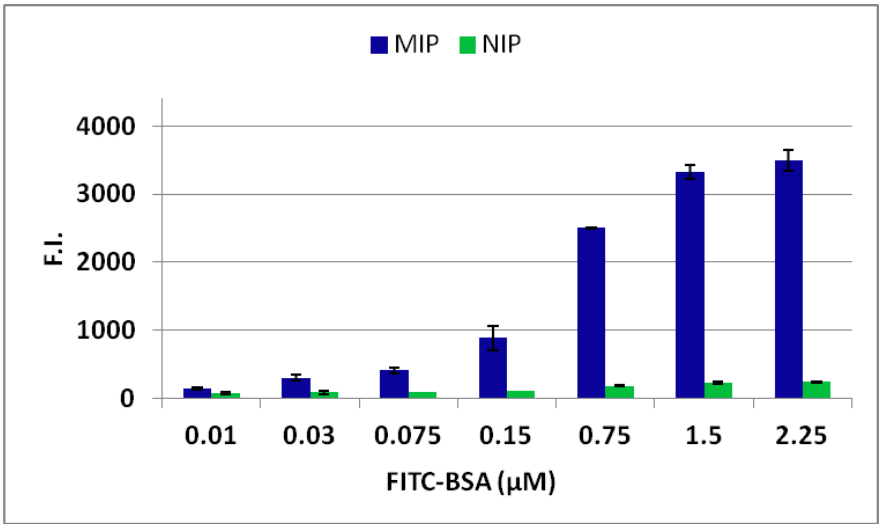

Figure 23. Histogram of fluorescence intensity of MIP and NIP.

As the figure 23 shows, at each protein concentrations, the fluorescent intensity, due to uptake of FITC-BSA within the polymer network, is higher for MIP compared to NIP. Already by low protein concentration (0.03 μM) a significant difference in binding behavior between MIP and NIP is observed. As the protein concentration increases, the amount of protein bound to the MIP enhances until reaching a saturation plateau. Therefore, once all the

available binding sites of MIP are occupied by the protein, a further increase in the protein concentration does not lead to an increase in the adsorption capacity. Differently, fluorescence intensity relative to the template amount bound to the NIP maintains constant and much lower all along the template concentration range.

These results clearly demonstrate an effective improvement of the adsorption capacity of MIP due to the formation of specific binding sites in the imprinting process. A bound ratio (amount of protein bound to MIP compared to NIP) greater than unity indicates that BSA was memorized within the MIP compared to a randomly polymerized network of the NIP (bound ratio is 8.4 at 0.15 μM). To note, the amount of template bound to NIP is due to randomly introduced, properly positioned functional groups.

Further, in order to evaluate the contribution of the assistant-peptide in improving the recognition properties, a comparison of the adsorption properties between MIP and MIP-SA-allyl-peptide was obtained. The figure 24 shows a histogram of the fluorescence intensity correlated to the template amount bound to the network for MIP-SA-allyl-peptide, MIP, NIP-SA-allyl-peptide and NIP.

As the protein concentration increases, the fluorescence intensity both for MIP and MIP-SA-allyl-peptide enhances. At low concentrations no significant differences in template amounts bound to the polymer are observed between MIP and MIP-SA-allyl-peptide. However, starting from 0.15 μM, higher differences begin to emerge. NIP-SA-allyl-peptide on the other hand, shows a trend similar to NIP, with a much lower fluorescence intensity compared with both imprinted polymers.

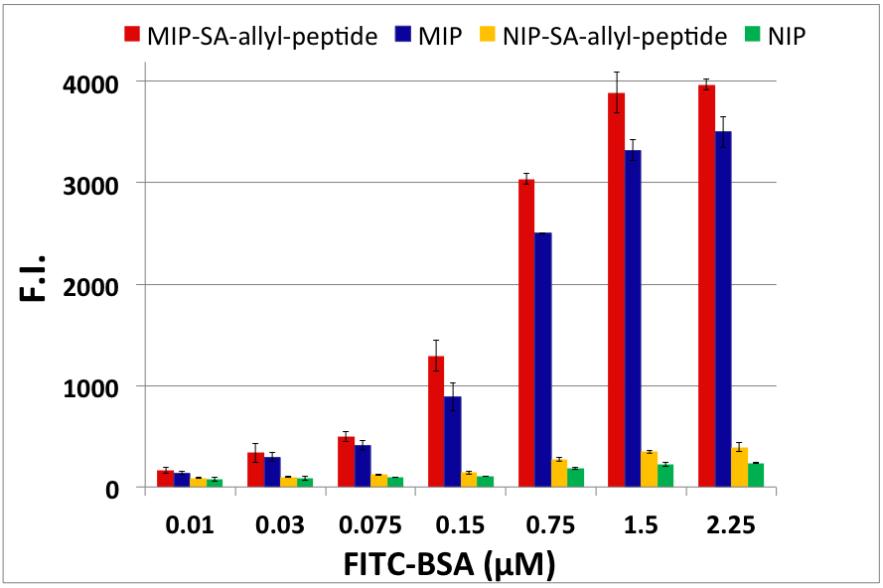

Figure 24. Histogram of fluorescence intensity of MIP-SA-allyl-peptide, MIP, NIP-SA-allyl-peptide and NIP.

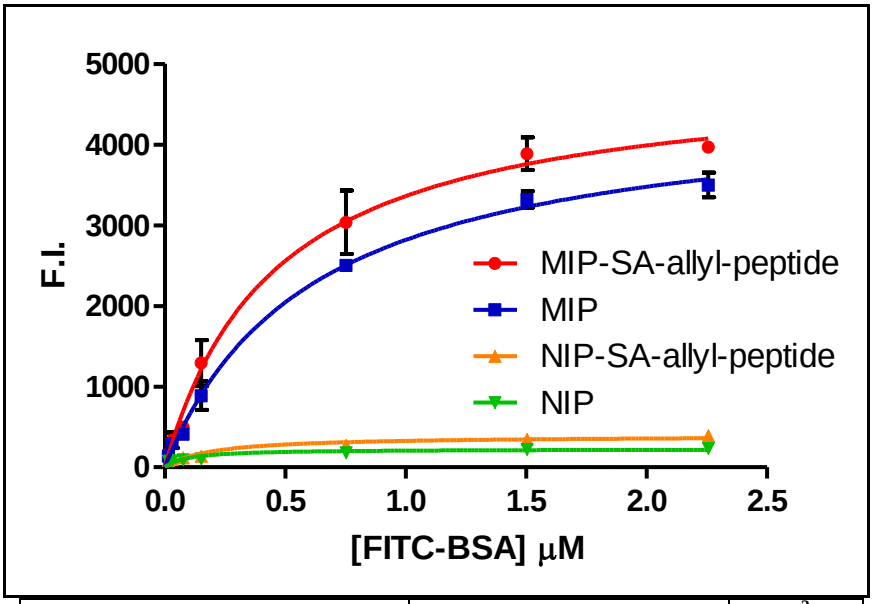

	K_D (μM)	R^2
MIP-SA-allyl-peptide	0.45 ± 0.06	0.9957
MIP	0.61 ± 0.06	0.9978

Figure 25. Fitting curves of MIP-SA-allyl-peptide, MIP, NIP-SA-allyl-peptide and NIP in the upper part of the figure; table with corresponding dissociation constants of MIP-SA-allyl-peptide and MIP in the lower part of the figure.

By fitting the overall data to a non-linear specific binding isotherm, fitting curves provided dissociation constants for each polymer (figure 25).

Both MIP and MIP-SA-allyl-peptide show dissociation constants (K_D) in the same order of magnitude of those reported in literature, which range from 0.01 to 1000 μM [4]. In particular, MIP-SA-allyl-peptide shows a K_D lower than MIP, indicating a higher affinity of MIP-SA-allyl-peptide for BSA. The K_D of NIP and NIP-SA-allyl-peptide are not shown because the binding model does not fit the data. This bacause the F.I. for NIP and NIP-SA-allyl-peptide at increasing BSA concentrations do not follow a dose-response behaviour.

Although the difference in the dissociation constants between MIP and MIP-SA-allyl-peptide is not very remarkable, however these results give the evidence that the introduction of an assistant-peptide - SA-allyl-peptide - into the polymer network could enhance the recognition properties of MIP-SA-allyl-peptide compared with those of pure MIP. Furthermore, as the NIP-SA-allyl-peptide show a slighly greater absorption behaviour compared with NIP, it meas that the peptide needs the protein to impart affinity to the polymer. Thus the assistant-peptide co-operates with the protein in imprinting the cavity. The specific assembly of the peptide with the protein in the pre-polymerization solution allows for a stable and high affinity complex. Functional and crosslinker monomers also participate in the interactions with the complex and, upon polymerization, immobilized the peptide into to the cavity. After removal of the template, assistant-peptide remained

immobilized into the cavity and acts as binding site for protein. So in this context, the peptide improved the recognition properties of MIP-SA-allyl-peptide not only by providing high affinity assembly with the protein, but also as assistant-monomer in the "freezing" of the pre-polymerization assembly. In other words the peptide acts as a specific extension of the functional and crosslinking monomers. The purpose of adding the functional and crosslinking monomers is to participate in the interactions with the complex, immobilize the assistant-peptide within the cavity, form the cross-linked polymeric network as well as provide a mechanical support to the polymer itself.

4.2.2.4.2. Kinetic binding studies

The time for equilibrium to occur in MIPs and NIPs was predetermined by kinetic binding studies where polymer samples were taken at different time points and analyzed by confocal fluorescence microscopy. Furthermore, the kinetic studies were performed to measure a K_D and compare this with K_D from equilibrium studies. The figure 25 shows the raw data of fluorescence intensity for three BSA concentrations at each time point of MIP-SA-allyl-peptide and MIP.

By fitting the data with an exponential association equation, observed rate constants (K_{ob}) at each concentration are obtained (table 13). As shown, the K_{ob} for MIP-SA-allyl-peptide and MIP increased with the concentration of BSA, so that the data fit with the model.

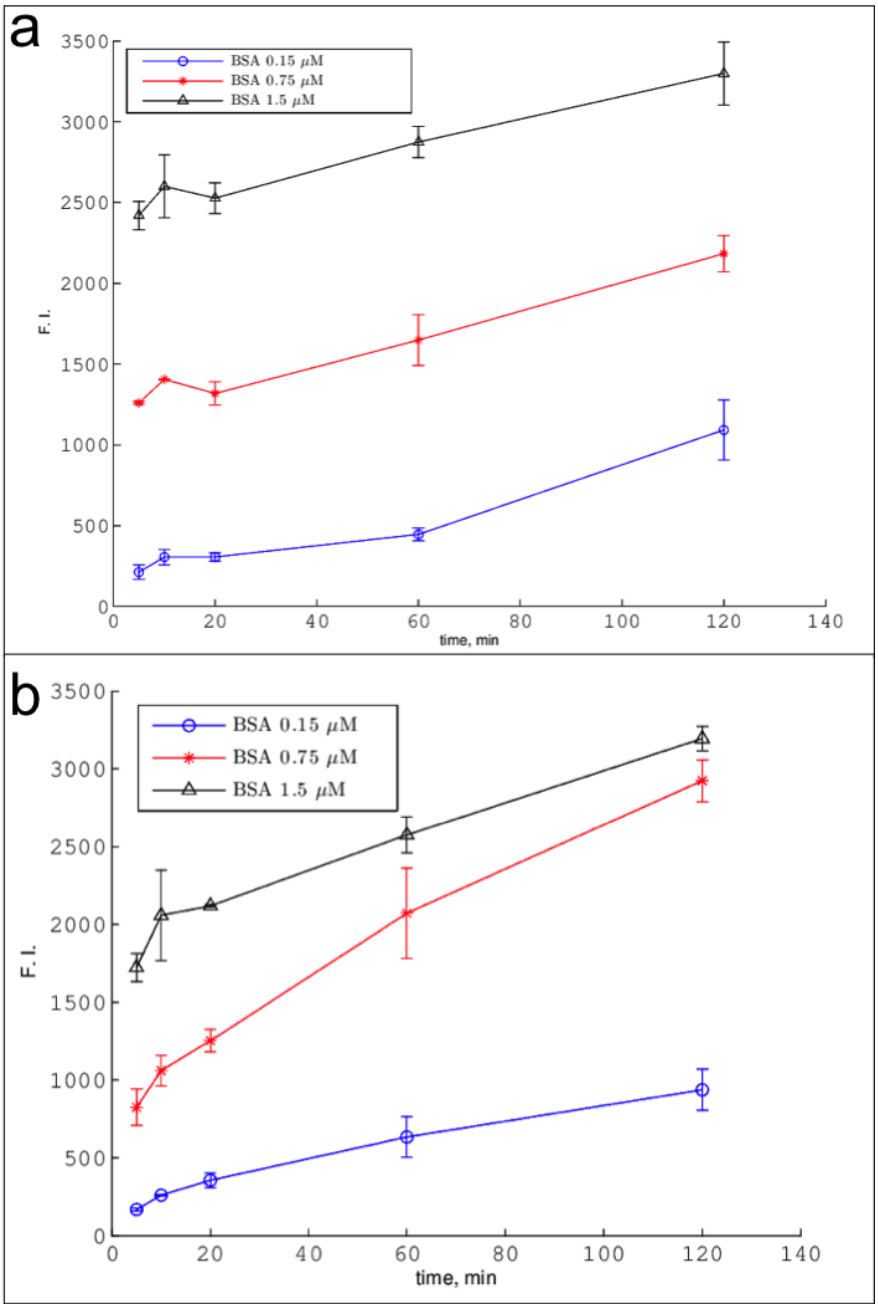

Figure 26. Fluorescence intensity for three BSA concentrations at each time point of a) MIP-SA-ally-peptide and b) MIP.

On the contrary, the same equation does not fit the data of NIP-SA-ally-peptide and NIP: K_{ob} do not increase with the concentration of BSA and the associated R^2 are very low. By fitting the as-obtained K_{ob} of MIP-SA-allyl-peptide and MIP with a linear equation, dissociation constants (K_D) are calculated. As the K_D of MIP-SA-allyl-dansyl-peptide is lower than MIP, it means that MIP-SA-allyl-peptide has much affinity for BSA for the reasons already discussed in section 4.2.2.4.1. Although these K_D do not match the K_D calculated from equilibrium binding studies, the affinity trend of MIP-SA-allyl-peptide and MIP is maintained. However, a similar discrepancy between the K_D calculated from equilibrium binding studies compared to kinetic binding analysis was already demonstrated by Sullivan [96].

	BSA (µM)	**K_{ob} (min^{-1})**	**R^2**	**K_D (µM)**
MIP-SA-allyl-dansyl-peptide	0.15	0.0090	0.8597	2.86
	0.75	0.0127	0.8991	
	1.5	0.0135	0.9355	
MIP	0.15	0.0156	0.9907	5.09
	0.75	0.0175	0.9803	
	1.5	0.0196	0.9429	
NIP-SA-allyl-dansyl-peptide	0.15	0.0065	0.9987	no fit
	0.75	9.7300	0.4211	
	1.5	0.0143	0.8910	
NIP	0.15	10.0500	0.1835	no fit
	0.75	no fit	no fit	
	1.5	0.1580	0.0861	

Table 13. Fitting data of kinetic binding studies.

4.2.2.5. Competitive binding studies

In order to characterize the selectivity of MIPs toward others proteins, competitive binding studies were performed. A fix amount

of fluorescent BSA conjugate (FITC-BSA) was added to increasing amounts of competitor proteins (BSA, LYS, OVA). Then, fluorescence microscopy images of the polymers following the binding were collected (figure 27).

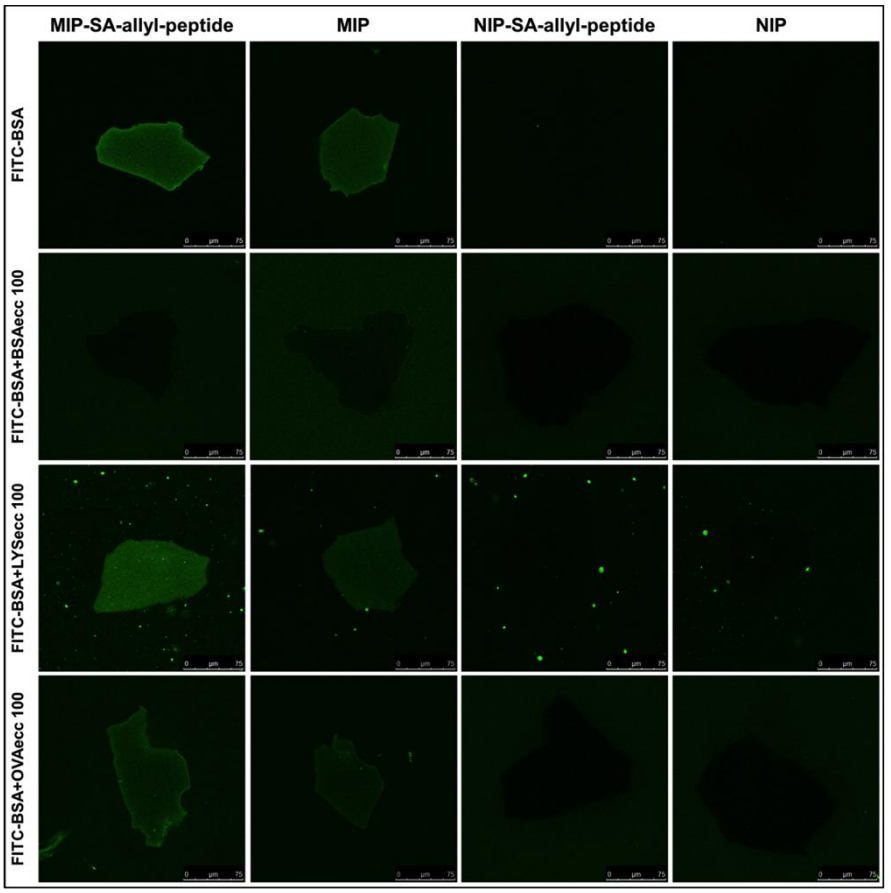

Figure 27. Fluorescence microscopy images of single microparticle of MIP-SA-allyl-peptide, MIP, NIP-SA-allyl-peptide and NIP added to a fix amount of FITC-BSA with a 100-fold excess of competitor proteins (BSA, LYS, OVA).

By analyzing fluorescence intensity from each polymer, a quantitative analysis of the binding was obtained. As the concentration of the competitor proteins increased and FITC-BSA is

held at constant concentration, the fluorescence intensity on MIP and MIP-SA-allyl-peptide show different behaviors.

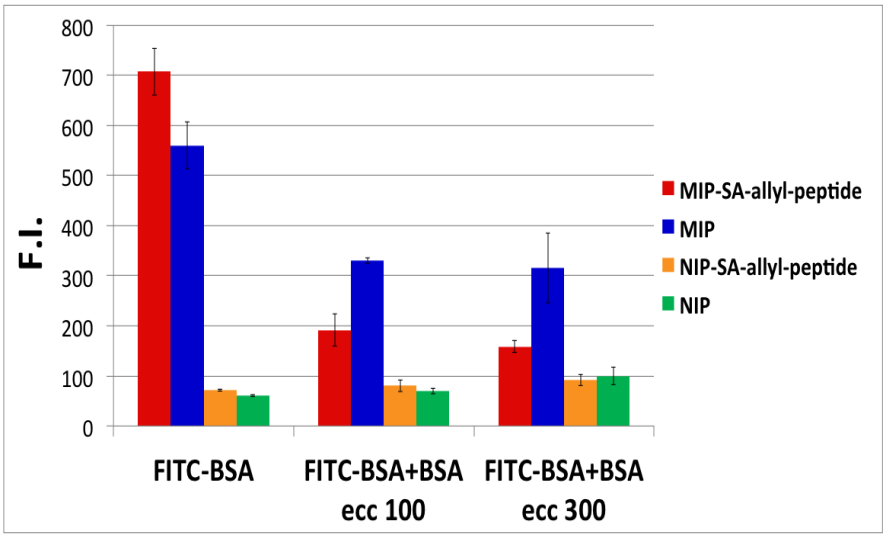

Figure 28. Comparison of fluorescence intensity of MIP-SA-allyl-peptide, MIP, NIP-SA-allyl-peptide and NIP in presence of a fix amount of FITC-BSA added to varying amount of BSA competitor protein.

In presence of 100- and 300-fold excess of BSA, the fluorescence intensity on MIP decreases of 1.7 and 1.8 times, respectively (figure 28). At the same conditions instead, on MIP-SA-allyl peptide the fluorescence intensity decreases much more. On the other hand, NIP and NIP-SA-allyl-peptide show no selectivity toward BSA. The decrease of fluorescence can be attributed to BSA that competes and occupies the binding sites once occupied by FITC-BSA. As the fluorescence intensity decrease is greater for MIP-SA-allyl-peptide than for MIP, it demonstrates that the sites formed on MIP-SA-allyl-peptide matched much better in size and charge with BSA than those on MIP.

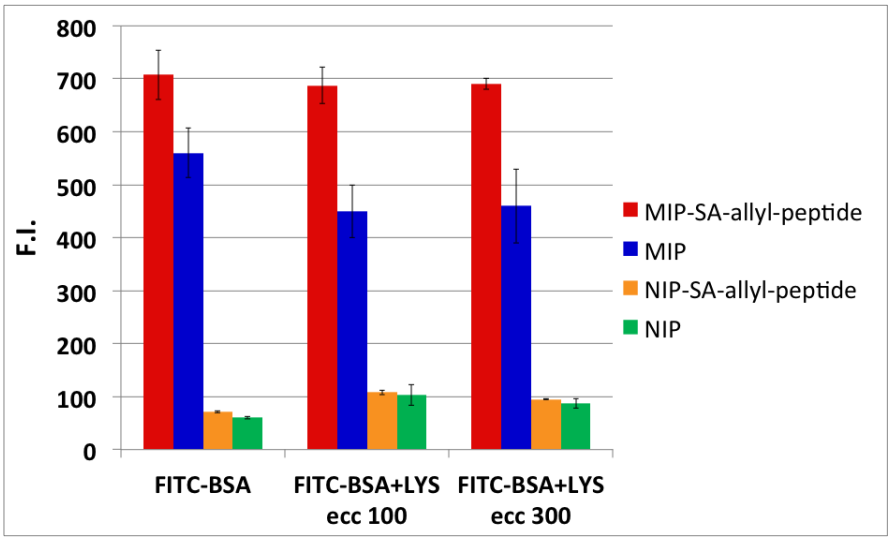

Figure 29. Comparison of fluorescence intensity of MIP-SA-allyl-peptide, MIP, NIP-SA-allyl-peptide and NIP in presence of a fix amount of FITC-BSA added to varying amount of LYS competitor protein.

In presence of LYS, fluorescence intensity on MIP decreases of 1.2 times, while on MIP-SA-allyl-peptide remained approximately unchanged (figure 29). Although LYS has a smaller steric hindrance than BSA, and could easily occupy the binding sites, however LYS has a superficial charge much positive. So, the access of LYS to the imprinted sites of MIP-SA-allyl-peptide is prevented by the differences of charges between the imprinted cavity and LYS and therefore no significant fluorescence intensity changes are observed. Finally, in presence of a 100- and 300-fold excess of OVA the fluorescence intensity on MIP decreases of 1.6 and of 1.8 times while on MIP-SA-allyl-peptide decreases of 1.3 times (figure 30). Both imprinted-polymers, and in particular MIP-SA-allyl-peptide shows smaller decrease than that observed in presence of BSA. It suggests that the imprinted cavity is able to distinguish the slight differences in the protein structure between BSA and OVA.

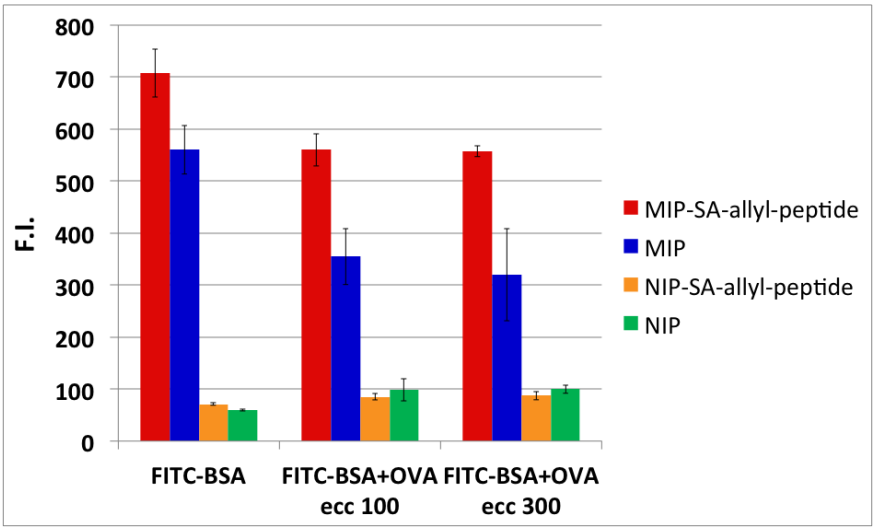

Figure 30. Comparison of fluorescence intensity of MIP-SA-allyl-peptide, MIP, NIP-SA-allyl-peptide and NIP in presence of a fix amount of FITC-BSA added to varying amount of OVA competitor protein.

The overall results of the competitive studies clearly demonstrate that MIP and MIP-SA-allyl-peptide shown selectivity values in the same order of magnitude of those reported in literature which range from 1 to 8 [93]. To date, MIP-SA-allyl-peptide is more selective than MIP. MIP-SA-allyl-peptide is selective toward BSA even at low concentrations (100-fold excess BSA), is selective toward LYS until high concentrations (300-fold excess LYS) and is selective, but in lesser extent, to OVA. The greater ability of MIP-SA-allyl-peptide compared to MIP to distinguish the differences between the competitor proteins is due to the assistant-peptide that was positioned into the cavity by the imprinting process and suitably oriented for the binding. Table 14 resumes selectivity of MIP-SA-allyl-peptide and MIP for the competitor proteins.

	excess competitor protein	Selectivity	
		MIP-SA-allyl-peptide	MIP
BSA	100	3.7	1.7
	300	4.5	1.8
LYS	100	1.0	1.2
	300	1.0	1.2
OVA	100	1.3	1.6
	300	1.3	1.8

Table 14. Selectivity of MIP-SA-allyl-peptide and MIP toward competitor proteins (BSA, LYS, OVA).

4.2.2.6. Transduction signaling studies

In order to study the signaling functionality of MIP-SA-allyl-dansyl-peptide when bounded BSA, a fluorescence microscopy analysis was performed.

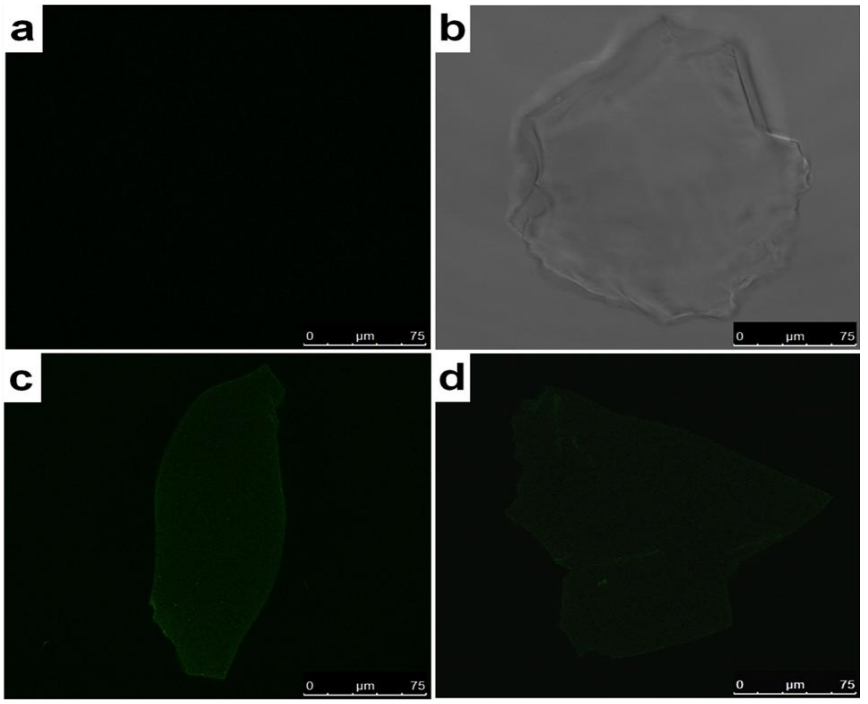

Figure 31. Comparison of (a) fluorescent channel of MIP-SA-allyl-peptide, (b) bright field of MIP-SA-allyl-peptide, (c) fluorescent channel of MIP-SA-allyl-dansyl-peptide and (d) fluorescent channel of MIP-SA-allyl-dansyl-ctrl(-)peptide.

The comparison of fluorescent-MIPs (MIP-SA-allyl-dansyl and MIP-SA-allyl-ctrl(-)peptide) with the non-fluorescent MIPs (MIP-SA-allyl-peptide) was shown in figure 31. The figure shows that both fluorescent-MIPs are clearly brighter in comparison to non-fluorescent MIP, demonstrating that fluorescent-SA-peptides were successfully polymerized into the polymer backbone during the imprinting process. The incorporation of the fluorescent-SA-peptides was due to the derivation of the fluorescent-SA-peptides with polymerizable allyl moiety that allow the immobilization into the polymer. However, the fluorescence of MIP-SA-allyl-dansyl-peptide is greater than that of MIP-SA-allyl-dansyl-ctrl(-)peptide. This difference could be explicate by the fact that the environment of dansyl is most likely different in MIP-SA-allyl-dansyl-peptide and MIP-SA-allyl-dansyl-ctrl(-)peptide, so the resultant fluorescence intensities are slightly different.

To evaluate the transduction signaling function, fluorescent-MIPs were added to increasing concentrations of BSA and the resultant fluorescence intensity changes were measured. As shown in figure 32, the fluorescence intensity of MIP-SA-ally-dansyl-peptide in absence of BSA was greater than the corresponding control polymer (NIP-SA-allyl-dansyl-peptide). Lower fluorescence intensities but with similar trend were observed for MIP-SA-allyl-ctrl(-)peptide and corresponding control polymer (NIP-SA-allyl-ctrl(-)peptide). The difference in fluorescence intensity in absence of BSA between imprinted and non-imprinted polymers can be attributed, as already explicated in this itself section, to a different environment in which the fluorescent-SA-peptides are.

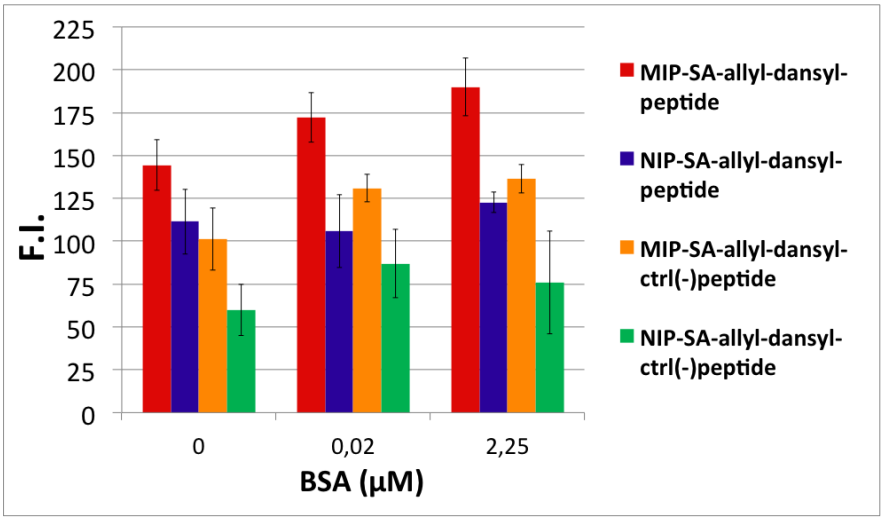

Figure 32. Fluorescence intensity of fluorescent-MIPs and fluorescent-NIPs in absence and presence of increasing concentrations of BSA.

By adding a BSA solution (0.02 µM), the fluorescence intensity of fluorescent-MIPs increases while that of fluorescent-NIPs remains quite constant. However, the increasing for MIP-SA-allyl-dansyl-peptide compared with MIP-SA-allyl-dansyl-ctrl(-)peptide is greater. By further increasing the BSA concentration to 2.26 µM, the fluorescence intensity on MIP-SA-allyl-dansyl-peptide enhances while on MIP-SA-allyl-ctrl(-)peptide remains constant. In summary, MIP-SA-allyl-dansyl-peptide shows dose-response behaviour. On the contrary, MIP-SA-allyl-ctrl(-)peptide as well as both fluorescent-NIPs do not show a similar trend and no significant fluorescence changes are observed upon addition of BSA.

These results indicate that the fluorescence change of MIP-SA-allyl-dansyl-peptide was due to the specific binding of BSA to the imprinted cavities, where SA-allyl-dansyl-peptide oriented suitably for BSA binding. The binding leads to great changes in the microenvironment of the fluorescent-SA-peptides localized inside

the imprinted cavity and to a corresponding enhancement of the fluorescence intensity. These results are in accordance with the spectroscopy studies discussed in section 4.1.2.4: the titration of SA-allyl-dansyl-peptide with BSA leads to a considerable increase of fluorescence intensity, while SA-allyl-dansyl-ctrl(-)peptide does not produce significant fluorescence changes.

By fitting the fluorescence intensity of MIP-SA-allyl-peptide against the concentration of BSA with a linear equation, a dose-response curve was obtained (figure 33).

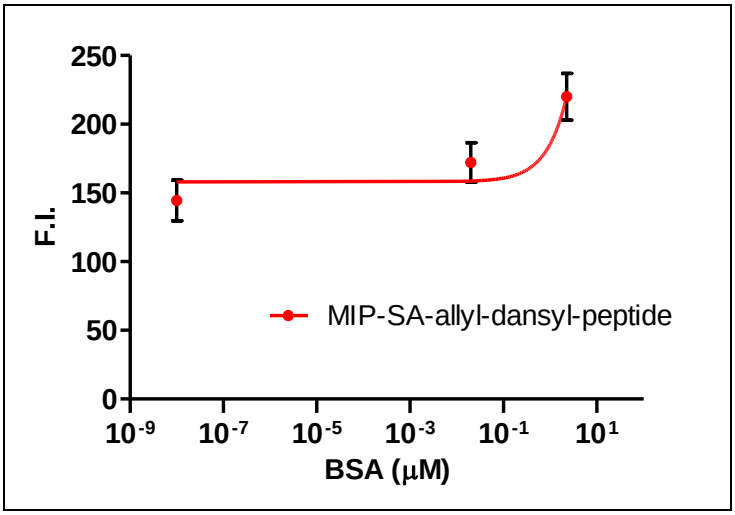

Figure 33. Dose-response curve for a logarithmic scale showing the fluorescence signal from MIP-SA-allyl-peptide in response to increasing concentrations of BSA.

The dose-response curve shows that MIP-SA-allyl-peptide is able to detect BSA over the concentration range between 0.00 and 2.25 μM. This curve represents a tool for a direct correlation of the fluorescence signal in response to increasing concentrations of BSA, providing the MIP-SA-allyl-dansyl-peptide of biosensor features.

Chapter 5. Conclusions

In conclusion, a molecularly imprinted polymer capable of signal transduction of protein binding event into a fluorescence change was synthesized using high affinity assistant-peptide bearing fluorescent probe.

For this purpose, the assistant-peptide was derivatized with an allyl-function to allow the immobilization into the polymer network. ITC analysis confirmed the maintenance of the recognition properties between BSA and the modified assistant-peptide.

Then, the assistant-peptide was incorporated into the polymer by a facile synthesis involving the assembly of the assistant-peptide with the BSA, the addition of the functional monomers and subsequent polymerization of the overall complex. Efficiency of template removal and chemical composition of the resultant polymers were confirmed by spectroscopic techniques.

The recognition properties were tested by fluorescence microscopy and proved that MIP-SA-allyl-peptide has large absorption capacity, good affinity and selectivity toward BSA when compared with pure MIP. These improvements were found to derive from the assistant-peptide that remains covalently immobilized and suitably oriented into the cavity, acting in cooperation with the imprinted-cavity as binding site for protein binding.

Furthermore, in order to provide MIP-SA-allyl-peptide of a signaling transduction function, the assistant-peptide was conjugated to an environment-sensitive fluorophore. Fluorescence titration of the environment-sensitive peptide with BSA resulted in

large emission changes compared with the negative control peptide, demonstrating the effectiveness of the peptide in reporting the binding.

Moreover, the environment-sensitive peptide was polymerized into the polymer network and the incorporation was demonstrated by fluorescence microscopy. The same technique was also used to verify the signaling transduction function of MIP-SA-allyl-dansyl-peptide. The results show fluorescence changes of MIP-SA-allyl-dansyl-peptide upon addition of BSA, demonstrating the ability of the polymer to report the protein binding event into a precise range of detection. The present work provides a new and general strategy for developing highly selective protein-imprinted polymers for biosensing purposes.

Chapter 6. References

[1] Bergmann, N. M., & Peppas, N. A. (2008). Molecularly imprinted polymers with specific recognition for macromolecules and proteins. *Progress in Polymer Science*, *33*(3), 271-288.

[2] Fischer E. (1894) Einfluss der configuration auf die wirkung derenzyme. Berichte der Deutschen Chemischen Gesellschaft (27), 2985-2993.

[3] Kryscio, D. R., & Peppas, N. A. (2012). Critical review and perspective of macromolecularly imprinted polymers. *Acta biomaterialia*, *8*(2), 461-473.

[4] Hilt, J. Z., & Byrne, M. E. (2004). Configurational biomimesis in drug delivery: molecular imprinting of biologically significant molecules. *Advanced drug delivery reviews*, *56*(11), 1599-1620.

[5] Chen, B., Piletsky, S., & Turner, A. P. (2002). Molecular recognition: design of "keys". *Combinatorial chemistry & high throughput screening*, *5*(6), 409-427.

[6] Hansen, D. E. (2007). Recent developments in the molecular imprinting of proteins. *Biomaterials*, *28*(29), 4178-4191.

[7] Wong, J., Chilkoti, A., & Moy, V. T. (1999). Direct force measurements of the streptavidin–biotin interaction. *Biomolecular engineering*, *16*(1), 45-55.

[8] Luong, J. H., Male, K. B., & Glennon, J. D. (2008). Biosensor technology: technology push versus market pull. *Biotechnology advances*, *26*(5), 492-500.

[9] Updike, S. J., & Hicks, G. P. (1967). The enzyme electrode. *Nature*, *214*, 986-988.

[10] Nakamura, H., & Karube, I. (2003). Current research activity in biosensors. *Analytical and bioanalytical chemistry*, *377*(3), 446-468.

[11] Higson, S. P., Reddy, S. M., & Vadgama, P. M. (1994). Enzyme and other biosensors: Evolution of a technology. *Engineering Science and Education Journal*, *3*(1), 41-48.

[12] Turner, A. P. (2000). Biosensors--sense and sensitivity. *Science*, *290*(5495), 1315-1317.

[13] Koyun, A., Ahlatcolu, E., & Koca, Y. (2012). Biosensors and their principles. *A Roadmap of Biomedical Engineers and Milestones*.

[14] Dixon, B. M., Lowry, J. P., & D O'Neill, R. (2002). Characterization in vitro and in vivo of the oxygen dependence of an enzyme/polymer biosensor for monitoring brain glucose. *Journal of Neuroscience Methods*, *119*(2), 135-142.

[15] Fan, X., White, I. M., Shopova, S. I., Zhu, H., Suter, J. D., & Sun, Y. (2008). Sensitive optical biosensors for unlabeled targets: A review. *analytica chimica acta*, *620*(1), 8-26.

[16] Thevenot, D. R., Toth, K., Durst, R. A., & Wilson, G. S. (1999). Electrochemical biosensors: recommended definitions and classification. *Pure and Applied Chemistry*, *71*(12), 2333-2348.

[17] Terry, L. A., White, S. F., & Tigwell, L. J. (2005). The application of biosensors to fresh produce and the wider food industry. *Journal of agricultural and food chemistry*, *53*(5), 1309-1316.

[18] Marazuela, M., & Moreno-Bondi, M. (2002). Fiber-optic biosensors–an overview. *Analytical and bioanalytical chemistry*, *372*(5-6), 664-682.

[19] Subrahmanyam, S., Piletsky, S. A., & Turner, A. P. (2002). Application of natural receptors in sensors and assays. *Analytical chemistry*, *74*(16), 3942-3951.

[20] Chambers, J. P., Arulanandam, B. P., Matta, L. L., Weis, A., & Valdes, J. J. (2008). *Biosensor recognition elements*. *Current Issues Molecular Biology.*

[21] Pazos, E., Vazquez, O., Mascarenas, J. L., & Vazquez, M. E. (2009). Peptide-based fluorescent biosensors. *Chemical Society Reviews*, *38*(12), 3348-3359.

[22] Kelly, D.,Xuedong, S., Daniel, F., Sergio, B. M., Nasser, P., Basil, I. S., Karen, M. G. (1999) Integrated optical toxin sensor. Boston, MA, 55-58.

[23] Williams, C., & Addona, T. A. (2000). The integration of SPR biosensors with mass spectrometry: possible applications for proteome analysis. *Trends in biotechnology*, *18*(2), 45-48.

[24] D'Orazio, P. (2011). Biosensors in clinical chemistry 2011 update. *Clinica Chimica Acta*, *412*(19), 1749-1761.

[25] Kojima, K., Witarto, A. B., & Sode, K. (2000). The production of soluble pyrroloquinoline quinone glucose dehydrogenase by Klebsiella pneumoniae, the alternative host of PQQ enzymes. *Biotechnology letters*, *22*(16), 1343-1347.

[26] Gooding, J. J., Pugliano, L., Hibbert, D. B., & Erokhin, P. (2000). Amperometric biosensor with enzyme amplification fabricated using self-assembled monolayers of alkanethiols: the influence of the spatial distribution of the enzymes. *Electrochemistry communications*, *2*(4), 217-221.

[27] Sapsford, K. E., Bradburne, C., Delehanty, J. B., & Medintz, I. L. (2008). Sensors for detecting biological agents. *Materials today*, *11*(3), 38-49.

[28] Moore, P., & Clayton, J. (2003). To affinity and beyond. *Nature*, *426*(6967), 725-731.

[29] Petrenko, V. A., & Sorokulova, I. B. (2004). Detection of biological threats. A challenge for directed molecular evolution. *Journal of microbiological methods*, *58*(2), 147-168.

[30] Conway, J. O., Sherwood, L. J., Collazo, M. T., Garza, J. A., & Hayhurst, A. (2010). Llama single domain antibodies specific for the 7 botulinum neurotoxin serotypes as heptaplex immunoreagents. *Plos one*, *5*(1), e8818.

[31] Ellington, A. D. & Szostak, J. W. (1990). In vitro selection of RNA molecules that bind specific ligands *Nature*, 346, 818-822.

[32] Jayasena, S. D. (1999). Aptamers: an emerging class of molecules that rival antibodies in diagnostics. *Clinical chemistry*, *45*(9), 1628-1650.

[33] Song, S., Wang, L., Li, J., Fan, C., & Zhao, J. (2008). Aptamer-based biosensors. *TrAC Trends in Analytical Chemistry*, *27*(2), 108-117.

[34] Lim, D. V., Simpson, J. M., Kearns, E. A., & Kramer, M. F. (2005). Current and developing technologies for monitoring agents of bioterrorism and biowarfare. *Clinical microbiology reviews*, *18*(4), 583-607.

[35] Pieken, W. A., Olsen, D. B., Benseler, F., Aurup, H., & Eckstein, F. (1991). Kinetic characterization of ribonuclease-resistant 2'-modified hammerhead ribozymes. *Science*, *253*(5017), 314-317.

[36] Ye, L., & Mosbach, K. (2008). Molecular imprinting: synthetic materials as substitutes for biological antibodies and receptors†. *Chemistry of Materials*, *20*(3), 859-868.

[37] Schneider, S., Buchert, M., Georgiev, O., Catimel, B., Halford, M., Stacker, S. A., Baechi, T., Moelling, K., Hovens, C. M. (1999). Mutagenesis and selection of PDZ domains that bind new protein targets. *Nature biotechnology*, *17*(2), 170-175.

[38] Cooper, W. J., & Waters, M. L. (2005). Molecular recognition with designed peptides and proteins. *Current opinion in chemical biology*, *9*(6), 627-631.

[39] DeGrado, W. F., Summa, C. M., Pavone, V., Nastri, F., & Lombardi, A. (1999). De novo design and structural characterization of proteins and metalloproteins. *Annual review of biochemistry*, *68*(1), 779-819.

[40] Lombardi, A., Marasco, D., Maglio, O., Di Costanzo, L., Nastri, F., & Pavone, V. (2000). Miniaturized metalloproteins: Application to iron–sulfur proteins. *Proceedings of the National Academy of Sciences*, *97*(22), 11922-11927.

[41] Pavan, S., & Berti, F. (2012). Short peptides as biosensor transducers. *Analytical and bioanalytical chemistry*, *402*(10), 3055-3070.

[42] Loving, G. S., Sainlos, M., & Imperiali, B. (2010). Monitoring protein interactions and dynamics with solvatochromic fluorophores. *Trends in biotechnology*, *28*(2), 73-83.

[43] Krueger, A. T., & Imperiali, B. (2013). Fluorescent amino acids: modular building blocks for the assembly of new tools for chemical biology. *ChemBioChem*, *14*(7), 788-799.

[44] Choulier, L., & Enander, K. (2010). Environmentally sensitive fluorescent sensors based on synthetic peptides. *Sensors*, *10*(4), 3126-3144.

[45] Polyakov, M. V. Adsorption properties and structure of silica gel (1931). *Zhur Fiz Khim*, 2, 799–805.

[46] Mosbach, K., & Ramström, O. (1996). The emerging technique of molecular imprinting and its future impact on biotechnology. *Nature Biotechnology*, *14*(2), 163-170.

[47] Pauling, L. (1940) A Theory of the Structure and Process of Formation of Antibodies. *Journal of the American Chemical Society*, (62)

[48] Whitcombe, M. J., Chianella, I., Larcombe, L., Piletsky, S. A., Noble, J., Porter, R., & Horgan, A. (2011). The rational development of molecularly imprinted polymer-based sensors for protein detection. *Chemical Society Reviews*, *40*(3), 1547-1571.

[49] Spivak, D. A. (2005). Optimization, evaluation, and characterization of molecularly imprinted polymers. *Advanced Drug Delivery Reviews*, *57*(12), 1779-1794.

[50] Li, S., Cao, S., Whitcombe, M. J., & Piletsky, S. A. (2014). Size matters: challenges in imprinting macromolecules. *Progress in Polymer Science*, *39*(1), 145-163.

[51] Byrne, M. E., Park, K., & Peppas, N. A. (2002). Molecular imprinting within hydrogels. *Advanced Drug Delivery Reviews*, *54*(1), 149-161.

[52] Ge, Y., & Turner, A. P. (2008). Too large to fit? Recent developments in macromolecular imprinting. *Trends in biotechnology*, *26*(4), 218-224.

[53] Arshady R, Mosbach K. Synthesis of substrate-selective polymers by host–guest polymerization. Makromol Chem 1981;182:687–92

[54] Bossi, A., Bonini, F., Turner, A. P. F., & Piletsky, S. A. (2007). Molecularly imprinted polymers for the recognition of proteins: the state of the art. *Biosensors and Bioelectronics*, *22*(6), 1131-1137.

[55] Byrne, M. E., & Salian, V. (2008). Molecular imprinting within hydrogels II: Progress and analysis of the field. *International journal of pharmaceutics*, *364*(2), 188-212.

[56] Verheyen, E., Schillemans, J. P., van Wijk, M., Demeniex, M. A., Hennink, W. E., & van Nostrum, C. F. (2011). Challenges for the effective molecular imprinting of proteins. *Biomaterials*, *32*(11), 3008-3020.

[57] Cormack, P. A., & Elorza, A. Z. (2004). Molecularly imprinted polymers: synthesis and characterisation. *Journal of Chromatography B*, *804*(1), 173-182.

[58] Liao, J. L., Wang, Y., & Hjertén, S. (1996). A novel support with artificially created recognition for the selective removal of proteins and for affinity chromatography. *Chromatographia*, *42*(5-6), 259-262.

[59] Hjerten, S., Liao, J. L., Nakazato, K., Wang, Y., Zamaratskaia, G., & Zhang, H. X. (1997). Gels mimicking antibodies in their selective recognition of proteins. *Chromatographia*, *44*(5-6), 227-234.

[60] Ghasemzadeh, N., Nyberg, F., & Hjertén, S. (2008). Highly selective artificial gel antibodies for detection and quantification of biomarkers in clinical samples. II. Albumin in body fluids of patients with neurological disorders. *Journal of separation science*, *31*(22), 3954-3958.

[61] Hirayama, K., Sakai, Y., & Kameoka, K. (2001). Synthesis of polymer particles with specific lysozyme recognition sites by a molecular imprinting technique. *Journal of applied polymer science*, *81*(14), 3378-3387.

[62] Matsunaga, T., Hishiya, T., & Takeuchi, T. (2007). Optimization of Functional Monomer Content in Protein Imprinted Polymers. *Analytical Letters*, *40*(14), 2633-2640.

[63] Zhanga, W., Qina, L., Hea, X. W., Lia, W. Y., Zhanga, Y. K. (2009). Novel surface modified molecularly imprinted polymer using acryloyl--cyclodextrin and acrylamide as monomers for selective recognition of lysozyme in aqueous solution. *Journal of Chromatography A*, (1216), 4560-4567.

[64] Bergmann, N. M. (2005) Molecularly Imprinted Polyacrylamide Polymers and Copolymers with Specific Recognition for Serum Proteins. Doctoral theses.

[65] Alvarez-Lorenzo, C., Hiratani, H., & Concheiro, A. (2006). Contact lenses for drug delivery. *American Journal of Drug Delivery*, *4*(3), 131-151.

[66] Venkatesh, S., Sizemore, S.P., Byrne, M.E. (2007). Biomimetic hydrogels for enhanced loading and extended release of ocular therapeutics. *Biomaterials*, 28(4), 717-24.

[67] Meot-Ner, M. (2005). The ionic hydrogen bond. *Chemical reviews*, *105*(1), 213-284.

[68] Nishino, H., Huang, C. S., & Shea, K. J. (2006). Selective protein capture by epitope imprinting. *Angewandte Chemie International Edition*, *45*(15), 2392-2396.

[69] Koch, S. J., Renner, C., Xie, X., & Schrader, T. (2006). Tuning Linear Copolymers into Protein- Specific Hosts. *Angewandte Chemie*, *118*(38), 6500-6503.

[70] Guo, M. J., Zhao, Z., Fan, Y. G., Wang, C. H., Shi, L. Q., Xia, J. J., Long, Y., Mi, H. F. (2006). Protein-imprinted polymer with immobilized assistant recognition polymer chains. *Biomaterials*, *27*(24), 4381-4387.

[71] Xia, J., Long, Y., Guo, M., Wang, Y., & Mi, H. (2009). Separation/enrichment of the low-content high molecular weight natural protein using protein-imprinted polymers with ARPCs. *Science in China Series B: Chemistry*, *52*(9), 1388-1393.

[72] Liu, D., Yang, Q., Jin, S., Song, Y., Gao, J., Wang, Y., & Mi, H. (2014). Core–shell molecularly imprinted polymer nanoparticles with assistant recognition polymer chains for effective recognition and enrichment of natural low-abundance protein. *Acta biomaterialia*, *10*(2), 769-775.

[73] Taguchi, H., Sunayama, H., Takano, E., Kitayama, Y., Takeuchi, T., (2015). Preparation of molecularly imprinted polymers for the recognition of proteins *via* the generation of peptide-fragment binding sites by semi-covalent imprinting and enzymatic digestion. *Analyst*, *140*, 1448-1452.

[74] Chou, P. C., Rick, J., & Chou, T. C. (2005). C-reactive protein thin-film molecularly imprinted polymers formed using a micro-contact approach. *Analytica chimica acta*, *542*(1), 20-25.

[75] Wan, W., Biyikal, M., Wagner, R., Sellergren, B., & Rurack, K. (2013). Fluorescent Sensory Microparticles that "Light up" Consisting of a Silica Core and a Molecularly Imprinted Polymer (MIP) Shell. *Angewandte Chemie International Edition*, *52*(27), 7023-7027.

[76] Henry, O. Y., Cullen, D. C., & Piletsky, S. A. (2005). Optical interrogation of molecularly imprinted polymers and development of MIP sensors: a review. *Analytical and bioanalytical chemistry*, *382*(4), 947-956.

[77] Ivanova Mitseva, P. K., Guerreiro, A., Piletska, E. V., Whitcombe, M. J., Zhou, Z., Mitsev, P. A., Davis, F., & Piletsky, S. A. (2012). Cubic molecularly imprinted polymer nanoparticles with a fluorescent core. *Angewandte Chemie International Edition*, *51*(21), 5196-5199.

[78] Rouhani, S., Nahavandifard, F. (2014). Molecular imprinting-based fluorescent optosensor using a polymerizable 1,8-naphthalimide dye as a florescence functional monomer. *Sensors and Actuators B Chemical*, *197*, 185-192.

[79] Takeuchi, T., Mukawa, T., & Shinmori, H. (2005). Signaling molecularly imprinted polymers: molecular recognition based sensing materials. *The Chemical Record*, *5*(5), 263-275.

[80] Zhang, W., He, X. W., Chen, Y., Li, W. Y., & Zhang, Y. K. (2011). Composite of CdTe quantum dots and molecularly imprinted polymer as a sensing material for cytochrome c. *Biosensors and Bioelectronics*, *26*(5), 2553-2558.

[81] Inoue, Y., Kuwahara, A., Ohmori, K., Sunayama, H., Ooya, T., & Takeuchi, T. (2013). Fluorescent molecularly imprinted polymer thin films for specific protein detection prepared with dansyl ethylenediamine-conjugated O-acryloyl l-hydroxyproline. *Biosensors and Bioelectronics*, *48*, 113-119.

[82] Deng, Q., Wu, J., Zhai, X., Fang, G., & Wang, S. (2013). Highly Selective Fluorescent Sensing of Proteins Based on a Fluorescent Molecularly Imprinted Nanosensor. *Sensors*, *13*(10), 12994-13004.

[83] Sunayama, H., Ooya, T., & Takeuchi, T. (2010). Fluorescent protein recognition polymer thin films capable of selective signal transduction of target binding events prepared by molecular imprinting with a post-imprinting treatment. *Biosensors and bioelectronics*, *26*(2), 458-462.

[84] Suga, Y., Sunayama, H., Ooya, T., & Takeuchi, T. (2013). Molecularly imprinted polymers prepared using protein-conjugated cleavable monomers followed by site-specific post-imprinting introduction of fluorescent reporter molecules. *Chemical Communications*, *49*(76), 8450-8452.

[85] Sunayama, H., Ooya, T., & Takeuchi, T. (2014). Fluorescent protein-imprinted polymers capable of signal transduction of specific binding events prepared by a site-directed two-step post-imprinting modification. *Chem. Commun.*, *50*(11), 1347-1349.

[86] Tao, Z., Tehan, E. C., Bukowski, R. M., Tang, Y., Shughart, E. L., Holthoff, W. G., Holthoff, W. G., Cartwright, A. N., Titus, A. H., Bright, F. V. (2006). Templated xerogels as platforms for biomolecule-less biomolecule sensors. *Analytica chimica acta*, *564*(1), 59-65.

[87] Dennis, M. S., Zhang, M., Meng, Y. G., Kadkhodayan, M., Kirchhofer, D., Combs, D., & Damico, L. A. (2002). Albumin binding as a general strategy for improving the pharmacokinetics of proteins. *Journal of Biological Chemistry*, *277*(38), 35035-35043.

[88] Putnam, F. W. (1975). Alpha, beta, gamma, omega-the roster of the plasma proteins. *The plasma proteins*, *1*, 57-130.

[89] Turcatti, G., Zoffmann, S., Lowe, J. A., Drozda, S. E., Chassaing, G., Schwartz, T. W., & Chollet, A. (1997). Characterization of non-peptide antagonist and peptide agonist binding sites of the NK1 receptor with fluorescent ligands. *Journal of Biological Chemistry*, *272*(34), 21167-21175.

[90] Kotrotsiou, O., Chaitidou, S., & Kiparissides, C. (2009). Boc-L-tryptophan imprinted polymeric microparticles for bioanalytical applications. *Materials Science and Engineering: C*, *29*(7), 2141-2146.

[91] Yan, H., & Row, K. H. (2006). Characteristic and synthetic approach of molecularly imprinted polymer. *International journal of molecular Sciences*, *7*(5), 155-178.

[92] Andac, M., Galaev, I. Y., & Denizli, A. (2013). Molecularly imprinted poly (hydroxyethyl methacrylate) based cryogel for albumin depletion from human serum. *Colloids and Surfaces B: Biointerfaces*, *109*, 259-265.

[93] Turner, N. W., Jeans, C. W., Brain, K. R., Allender, C. J., Hlady, V., & Britt, D. W. (2006). From 3D to 2D: a review of the molecular imprinting of proteins. *Biotechnology progress*, *22*(6), 1474-1489.

[94] Byrne, M. E., Hilt, J. Z., & Peppas, N. A. (2008). Recognitive biomimetic networks with moiety imprinting for intelligent drug delivery. *Journal of Biomedical Materials Research Part A*, *84*(1), 137-147.

[95] Hilt, J. Z., Byrne, M. E., & Peppas, N. A. (2006). Microfabrication of intelligent biomimetic networks for recognition of D-glucose. *Chemistry of materials*, *18*(25), 5869-5875.

[96] Sullivan, S. K., Hoare, S. R., Fleck, B. A., Zhu, Y. F., Heise, C. E., Struthers, R. S., & Crowe, P. D. (2006). Kinetics of non peptide antagonist binding to the human gonadotropin-releasing hormone receptor: implications for structure–activity relationships and insurmountable antagonism. *Biochemical pharmacology*, *72*(7), 838-849.

Appendix A

A1

SA-peptide crude

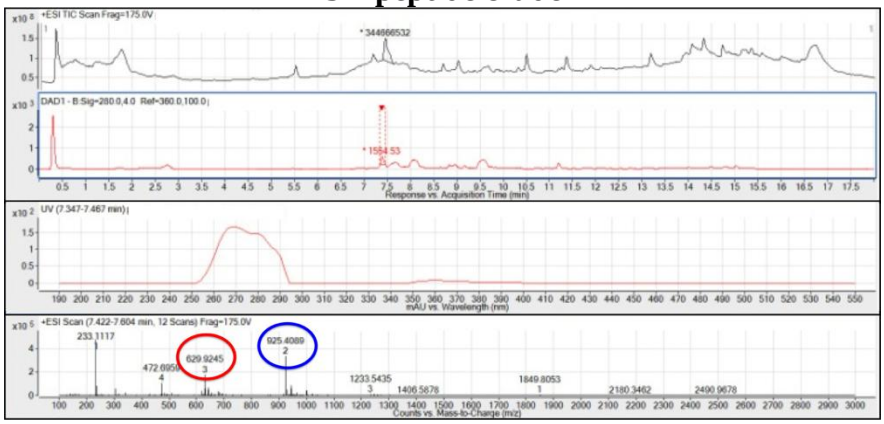

SA-peptide purified

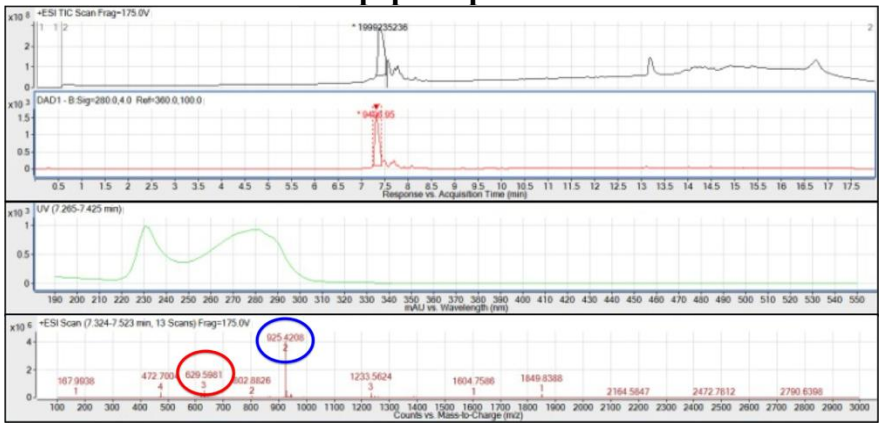

SA-peptide cyclized

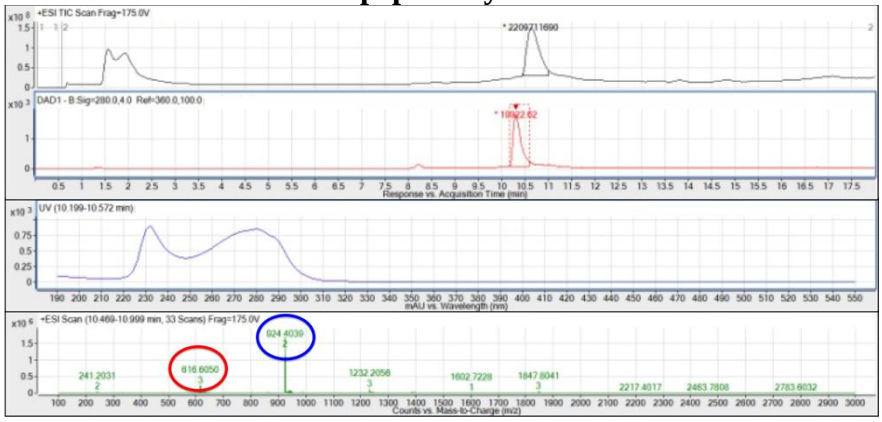

A2

SA-allyl-peptide crude

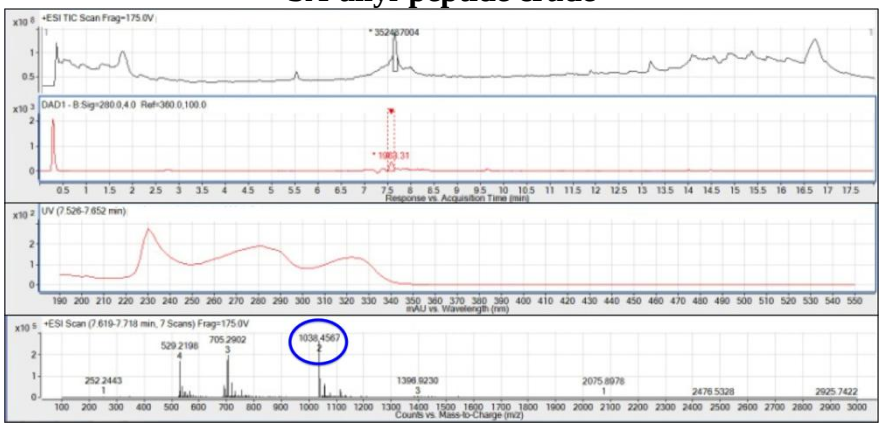

SA-allyl-peptide purified

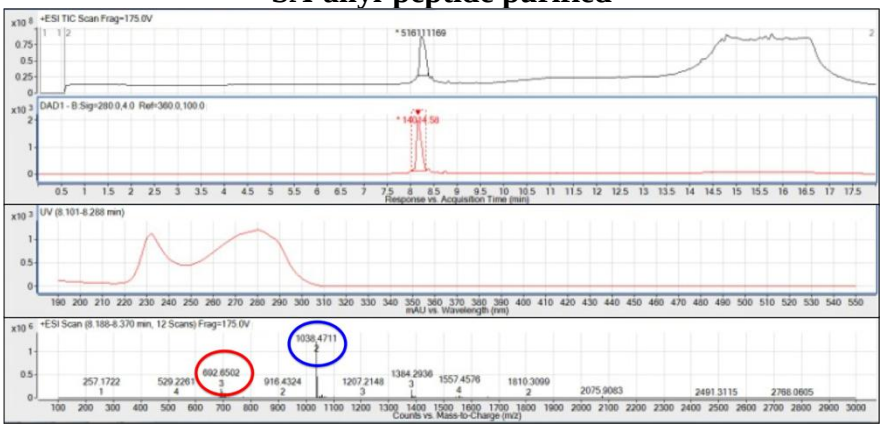

SA-allyl-peptide cyclized

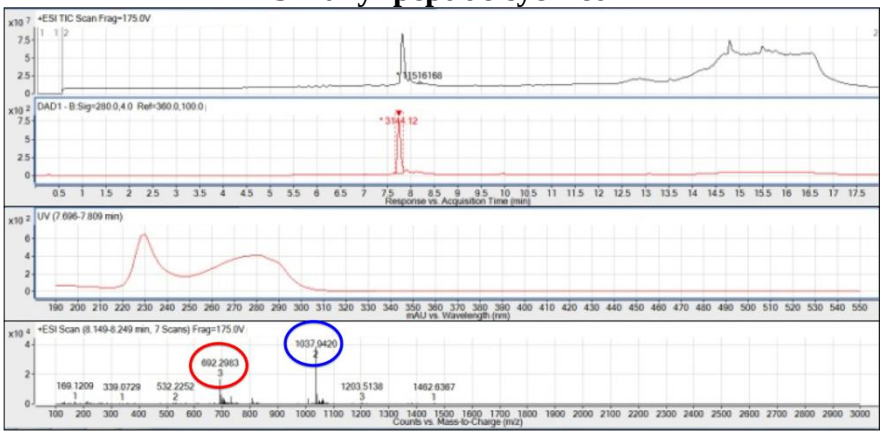

A3

SA-allyl-dansyl-peptide crude

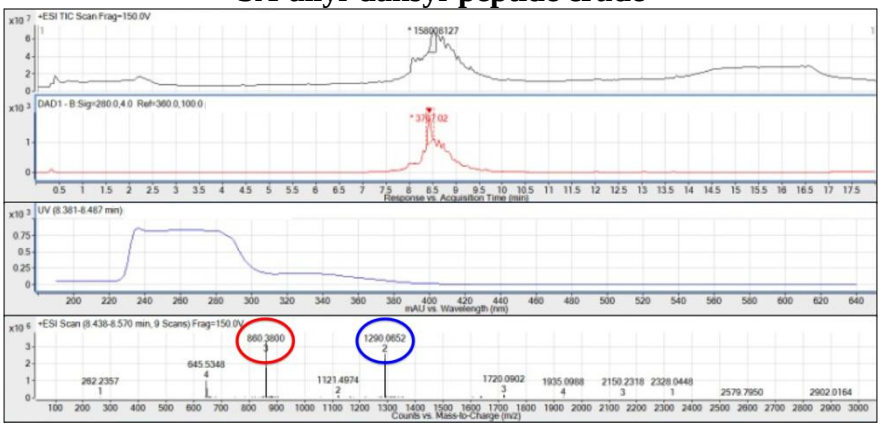

SA-allyl-dansyl-peptide purified

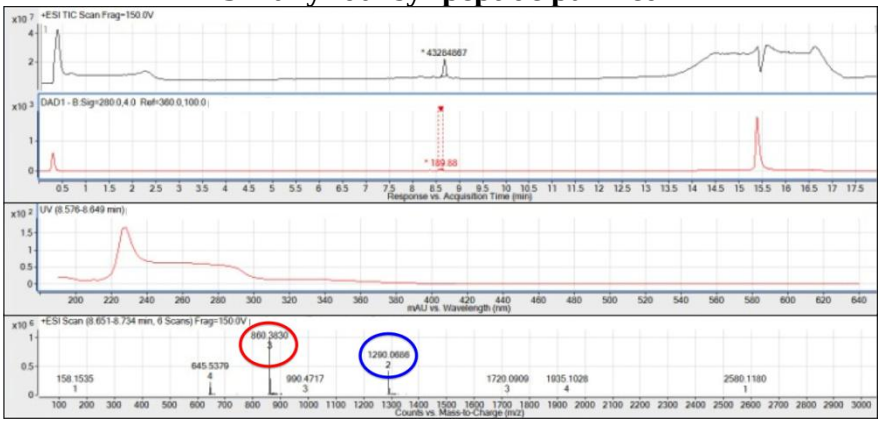

SA-allyl-dansyl-peptide cyclized

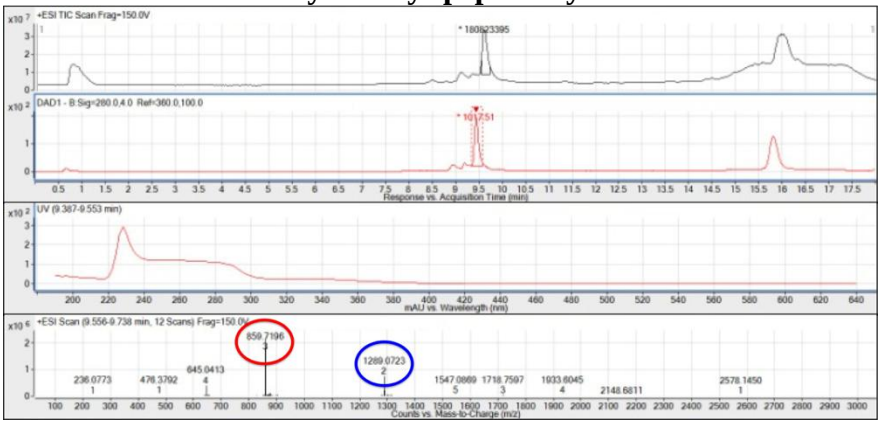

A4

SA-allyl-dansyl-ctrl(-)peptide crude

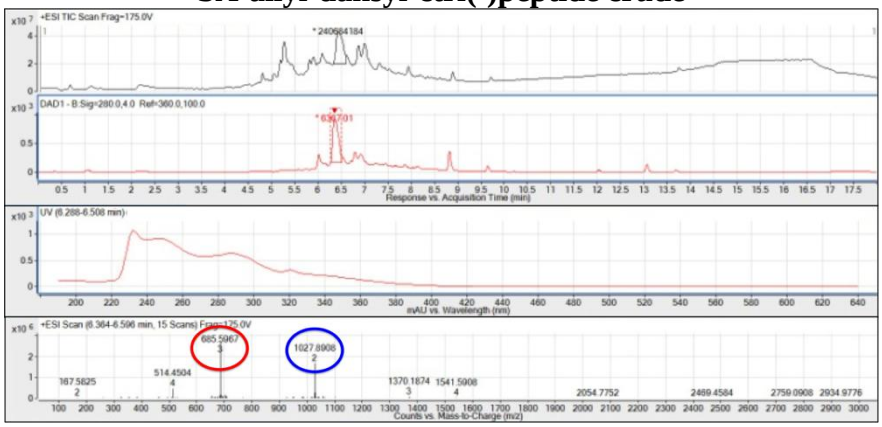

SA-allyl-dansyl-ctrl(-)peptide purified

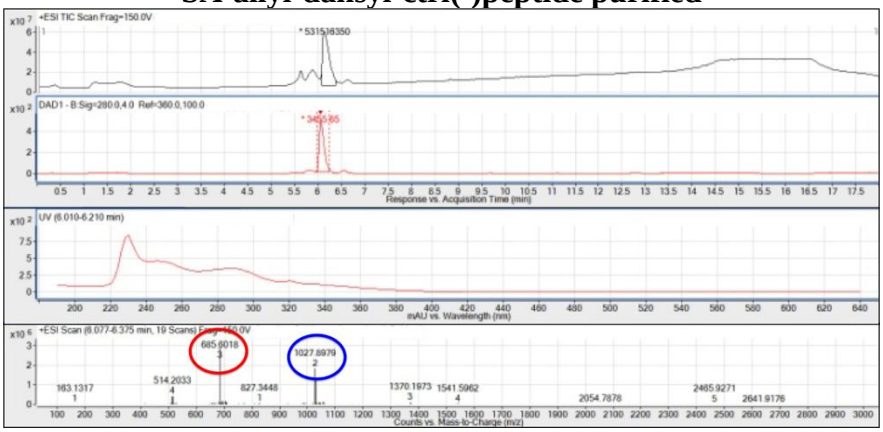

SA-allyl-dansyl-ctrl(-)peptide cyclized

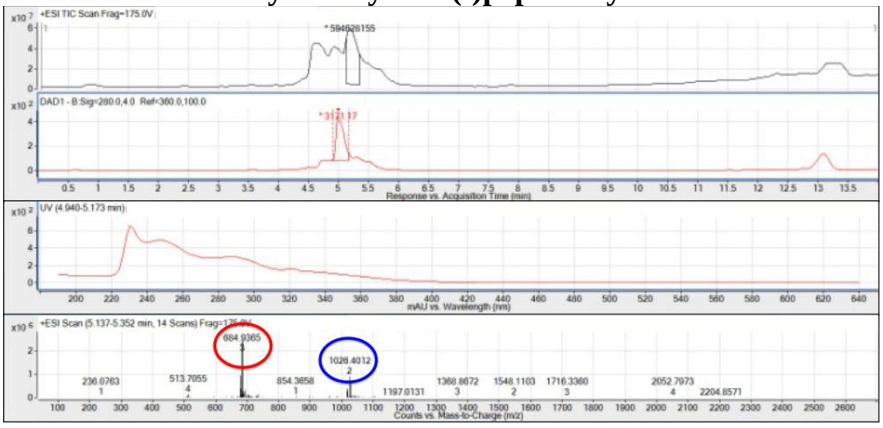

Figure 34. HPLC-MS characterization of (A1) SA-peptide, (A2) SA-allyl-peptide, (A3) SA-allyl-dansyl-peptide, (A4) SA-allyl-dansyl-ctrl(-)peptide. For each single peptide were reported the mass spectra of the crude products from peptide synthesis, the purified peptide and the cyclized peptide. The $[M/2]^{+2}$ and $[M/3]^{+3}$ fragment ion peaks in the ESI scan spectra were highlighted in blue and red, respectively.